



POWER ELECTRONICS STARTER FOR WOUND ROTOR INDUCTION MOTORS

A dissertation submitted to the
Department of Electrical Engineering, University of Moratuwa
in partial fulfilment of the requirements for the
Degree of Master of Science

By
WARSHA HANNEDIGE INDIKA DARSHANA SOYSA

Supervised by: Dr. J. P. Karunadasa.

Department of Electrical Engineering
University of Moratuwa
Sri Lanka

2010

94549



Abstract

Being the workhorse, induction motors are serving the industry. Mostly we can see squirrel cage motors, but when it's come to the large industries, wound rotor induction motors are also there. Applications like Mills, Large Fans, Pumps, Blowers, Crushers and Overhead Cranes which require higher starting torques use wound rotor induction motors to have a higher starting torque at a lower starting current at the stator. Generally wound rotor induction motors require more maintenance than squirrel cage motors because of its rotor construction, slip ring assembly and the starting method used.

Conventionally, wound rotor motors use an external resistor bank, which is connected to the rotor winding via slip rings, and external rotor resistance varies from a maximum value to zero as the rotor speed develops. Varying the external resistance can be achieved by several electromechanical methods. This is done in a stepwise manner with a motorized camshaft with electromechanical contact points or with a set of electrical power contactors and timers having a suitable time delay between adjacent steps. The traditional starter is highly mechanical and can cause lot of startup delays and is bulkier and requires frequent maintenance. To ensure right operation of rotor resistance control, the motor control circuit incorporates several additional measures and these are too prone to failures due to their own nature. Due to high heat dissipation in the resistors the number of consecutive startups during a short time period is also limited.

The proposed power electronic starter is entirely a power electronic device, which is having a three-phase rectifier bridge and a programmable transistor chopper. Programmable transistor chopper ensures a gradual speed development at rotor and control the acceleration with the duty factor of the transistor. This could eliminate the major disadvantage of traditional starter, which is the dependability of rotor speed with the load torque by extending it to have a closed loop speed control. Thereby we can ensure the programmable torque-speed characteristics with this power electronic



starter. This power electronic development will minimize the overall maintenance, and avoid current fluctuations completely during speed changes while demanding speed up or down at the rotor.

This report discusses the proposal, simulations in prone to the construction, hardware design and practical implementation and testing of starter with a no load wound rotor motor. Latter part of the report shows the performances of new starter over the conventional starter and future developments possible.

DECLARATION

The work submitted in this dissertation is the result of my own investigation, except where otherwise stated.

It has not already been accepted for any degree, and is also not being concurrently submitted for any other degree.

UOM Verified Signature

SOYSA. W.H.I.D.
30th January 2010

I endorse the declaration by the candidate.

UOM Verified Signature

Dr. J. P. Karunadasa.

Contents

Declaration	i
Contents	ii
Abstract	iv
Acknowledgement	v
List of Figures	vi
List of Tables	viii

Chapters

1. Introduction	1
1.1 Background	1
1.2 Motivation	2
1.3 Operation of WRIM with a Rotor Resistance Starter	2
1.4 Typical Nameplate data of WRIMs	2
2. Conventional Starters for WRIM	4
3. Proposed Power Electronic Starter	6
3.1 Power Block	6
3.2 Control Unit	8
4. Identifying Motor Parameters	9
4.1 Standard Tests	9
4.2 No Load Test	10
4.3 Locked Rotor Test	10
4.4 Identifying Motor Parameters with a VSD	11
5. Circuit Modeling and Simulation	14
5.1 Simulation – Set1	15
5.2 Simulation – Set2	18
5.3 Simulation – Set3	20
5.4 Simulation – Set4	22
5.5 Simulation – Set5	25
6. Selection of Power Semiconductors and Hardware Construction	28
6.1 Power Block	28
6.2 Three Phase Rectifier	29
6.3 Maximum Ratings and Characteristics of Diode Module	29
6.4 Calculation of Forward Current and Peak Inverse Voltage of Three-Phase Rectifier	30
6.5 Calculation of Collector Current and Collector-Emitter Voltage of IGBT	31
6.6 Transistor Chopper	31

6.7 Maximum Ratings and Characteristics of IGBT	31
6.8 Snubber Circuit	32
6.9 DC Link Commutating Choke	32
6.10 External Resistor	33
7. IGBT Gate Driver and Control Unit	34
7.1 Calculation of Gate Resistance	35
7.2 Characteristics of the Gate Driver	36
7.3 Control Unit	37
7.4 Source Code for HPWM Waveform Generation	39
8. Results and Discussion	41
8.1 Analysis of Rotor Currents	44
8.2 Analysis of Currents Waveform through the DC Link Commutation Choke	45
8.3 Harmonic Analysis	47
8.4 Analysis of Rotor Current Profiles with the FLUKE PQA	48
9. Comparison, Reliability of the System and Further Improvements	50
9.1 Power Electronics Starter vs. Conventional Starter	50
9.2 Reliability of the System	51
9.3 Programmable Torque-Speed Characteristics	51
9.4 Integration of Freewheeling Diode across the DC Commutation Choke	52
9.5 Advantages and Disadvantages of Power Electronics Starter over Conventional Starter	53
9.6 Advantages and Disadvantages of Power Electronics Starter over Variable Frequency Drivetric Theses & Dissertations	53
9.7 Conclusion	53
References	54
Annex	
Actual Figure of Implemented Power Electronics Starter	55

Acknowledgement

Thanks are due first to my supervisor, Dr. J. P. Karunadasa, for his great insights, perspectives, guidance and sense of humor. My sincere thanks go to the other staff members of the Electrical Engineering Department of University of Moratuwa, Sri Lanka for helping in various ways to clarify the things related to my academic works in time with excellent cooperation and guidance. Sincere gratitude is also extended to the people who serve in the Department of Electrical Engineering office.

In addition to that, I would like to extend my gratitude to the Plant management of Puttalam Cement Works, Holcim Lanka Ltd for providing me necessary support, material and labor requirement for construction of Power Electronics Starter.

Finally, I would like to thank many individuals, friends and colleagues who have not been mentioned here personally in making this educational process a success. May be I could not have made it without their supports.



University of Moratuwa, Sri Lanka.
Electronic Theses & Dissertations
www.lib.mrt.ac.lk

List of Figures

Figure	Page
Fig-1.1: Starting Current/ Torque vs. Speed of WRIM	2
Fig-2.1: Typical External Rotor Resistance Starter of WRIM	5
Fig-3.1: Proposed Power Electronics Starter for WRIM.....	6
Fig-3.2: Control Unit for Proposed Power Electronics Starter of WRIM	8
Fig-4.1: Carry out of No-Load-Test for 11kW WRIM.....	10
Fig-4.2: Carry out of Locked-Rotor-Test for 11kW WRIM.....	10
Fig-4.3: Modeling of the Equivalent Circuit Diagram of a Motor by the VSD.....	11
Fig-4.4: Identifying the Magnetizing Characteristics of the Motor.....	12
Fig-4.5: Perform Motor Identification Routine of a VSD for 11kW WRIM.....	12
Fig-4.6: Electrical Connections for 11kW WRIM to run with a VSD	12
Fig-5.1: Circuit Modeling with Matlab-Simulink.....	14
Fig-5.2: Ir-Rotor Current and Is-Stator Current Vs. Time [Pulse Freq. – 100Hz]	15
Fig-5.3: Closer look on Current Profiles of Rotor and Stator at D=75% [Pulse Freq. – 100Hz]	16
Fig-5.4: Rotor Speed Development with Different Duty Factors [Pulse Freq. - 100Hz]	17
Fig-5.5: Electromagnetic Torque Development with Different Duty Factors [Pulse Freq. – 100Hz]	17
Fig-5.6: Closer look on Current Profiles of Rotor and Stator [Pulse Freq. – 1kHz]	18
Fig-5.7: Closer look on Current Profiles of Rotor and Stator [Pulse Freq. – 5kHz]	19
Fig-5.8: Closer look on Current Profiles of Rotor and Stator [Pulse Freq. – 10kHz]	19
Fig-5.9: Speed and Torque Development of Rotor at 100Hz and 1kHz.....	20
Fig-5.10: Initial Current Profiles of Motor – Duty of IGBT = 0 and with connected Ext. Resistor Bridge.....	21
Fig-5.11: Final Current Profiles of Motor – Duty of IGBT = 1.....	21
Fig-5.12: Simulations without Inductor.....	22
Fig-5.13: Rotor and Stator Current Profiles without Inductor.....	23
Fig-5.14: Simulations without External Resistor.....	23
Fig-5.15: Rotor and Stator Current Profiles without External Resistor.....	24
Fig-5.16: Comparison of Rotor Speed Development vs. Time with Different External Resistances.....	24
Fig-5.17: Comparison of Torque Development of Rotor vs. Time with Different External Resistances.....	25
Fig-5.18: Modeled Power Electronics Starter in Simulink for Programmable Ramp Start	26
Fig-5.19: Comparison-Rotor Speed and Torque Development at Different Ramp-up Times	27
Fig-6.1: Actual Figure of a Power Block of Rotor Based Starter for 11kW WRIM	28
Fig-6.2: Schematic and Actual Figure of a Diode Module – Half Bridge.....	29
Fig-6.3: Electrical Circuit of the Power Electronics Starter for WRIM	30
Fig-6.4: Equivalent Circuit Schematic and Actual Figure of the IGBT Module.....	31
Fig-6.5: Switching Trajectory of the Gate Terminal and Current and Voltage Waveforms during Turn-On and Off.....	32

Fig-6.6: DC-Link Commutating Choke	33
Fig-6.7: Start Connected External High Pulse Resistors	33
Fig-7.1: Schematic of the IGBT Gate Drive Opto-coupler.....	34
Fig-7.2: Schematic of an Optimized Gate Driver Circuit with Output Discrete Stage.....	34
Fig-7.3: Schematic Diagram of an IGBT Gate Driver for Industrial VSD.....	35
Fig-7.4: Gate Resistance Calculation of the IGBT	35
Fig-7.5: Waveform of V_{GE} - PWM Signal for IGBT	36
Fig-7.6: Rise Time Calculation of Gate Signal of IGBT with the Oscilloscope	37
Fig-7.7: Fall Time Calculation of Gate Signal of IGBT with the Oscilloscope	37
Fig-7.8: Schematic Diagram of the Control Unit for the Power Electronics Starter of WRIM.....	38
Fig-7.9: Actual Figure of the Control Unit for the Power Electronics Starter of WRIM ..	38
Fig-8.1: Measuring Rotor Speed with a Digital Tachometer.....	41
Fig-8.2: Rotor Speed and V_{CE} vs. Duty Factor of IGBT	43
Fig-8.3: Current through IGBT and External Resistor vs. Duty Factor of IGBT	43
Fig-8.4: Rotor Current Profile with External Resistance.....	44
Fig-8.5: Rotor Current Profile at 20% of Duty Factor and Pulse Frequency of 5kHz	44
Fig-8.6: Rotor Current Profile at 40% of Duty Factor and Pulse Frequency of 5kHz	45
Fig-8.7: Rotor Current Profile at 80% of Duty Factor and Pulse Frequency of 5kHz	45
Fig-8.8: Current Profile through the DC Link Commutation Choke at 40% of Duty Factor and Pulse Frequency.....	46
Fig-8.9: Current Profile through the DC Link Commutation Choke at 100% of Duty Factor and Pulse Frequency of 10kHz.....	46
Fig-8.10: Electrical Connections of the Fluke Analyzer with WRIM	47
Fig-8.11: Harmonic Analysis of WRIM at 100% of Duty Factor and Pulse Frequency of 5kHz	48
Fig-8.12: Rotor Current Profile at 50% of Duty Factor and Pulse Frequency of 10kHz	49
Fig-8.13: Rotor Current Profile at 100% of Duty Factor and Pulse Frequency of 10kHz	49
Fig-8.14: Rotor Profile at 0% of Duty Factor and Pulse Frequency of 10kHz.....	49
Fig-9.1: Stator Current Profiles vs. Rotor Speed of an 11kW no load WRIM	50
Fig-9.2: Closed Loop Speed Control of a WRIM with Power Electronics Starter.....	51

List of Tables

Table	Page
Table-1.1: Typical Nameplate Data of WRIM	3
Table-4.1: Nameplate Data of 11kW WRIM.....	9
Table-4.2: Results of Standard Motor Tests for 11kW WRIM	10
Table-4.3: Identified Motor Parameters by the VSD for 11kW WRIM	13
Table-6.1: Ratings of Diode Module	30
Table-6.2: Maximum Ratings and Characteristics of IGBT	32
Table-8.1: Measuring of IGBT Collector Current, Current through External Resistor, V_{CE} and Rotor Speed vs. Duty Factor.....	42
Table-8.2: Harmonic Analysis at Different Duty Factors and Pulse Frequency of 5kHz	47
Table-8.3: Harmonic Analysis at different Pulse Frequencies	47



University of Moratuwa, Sri Lanka.
Electronic Theses & Dissertations
www.lib.mrt.ac.lk

Chapter 1

Introduction

Three-phase induction motors, the workhorse of the industry, and can be classified into two main groups based on their rotor construction as wound rotor induction motors (WRIM) and squirrel cage induction motors. Applications like Mills, Large Fans, Pumps, Blowers, Crushers and Overhead Cranes, which require higher starting torques, use WRIM to have a lower inrush current at the stator. Generally the WRIM requires more maintenance than the squirrel cage motor depending on its rotor construction, slip ring assembly and the starting method used.

Varying the external resistance connected to the rotor circuit via slip rings from a maximum value to zero while the rotor accelerates towards full speed normally does starting of a WRIM. This is done in a stepwise manner with a motorized camshaft with contact points or with a set of power contactors and timers having a suitable time delay between adjacent steps.

The operation of this traditional starter is highly mechanical and can cause lot of startup delays. It is bulky and requires frequent maintenance. To ensure right operation of rotor resistance control, the motor control circuit incorporates several additional measures and these are too prone to failures due to their own nature. Sensing of external rotor resistance min-max positions is very important to ensure the right operation of the motor starter. Due to high heat dissipation in the resistors the number of consecutive startups during a short time period is also limited.

Major disadvantage of a traditional starter is that the rotor speed, due to step-wise changes of the external rotor resistance, is highly dependent on load torque and the speed control capability of the motor is not up to the satisfactory level.

Altogether, stator current fluctuations when changing rotor resistance, unavailability of smooth speed increase, high dependence of speed variation on load torque, requirement of frequent maintenance for starter circuit and frequent starter failures during startups are the main disadvantages of the traditional external rotor resistance starter.

The power electronics starter proposed here can replace the traditional starter and provide the advantages of step-less smooth speed increase, programmable torque-speed characteristics, less maintenance and a higher reliability.

1.1 Background:

Application of WRIMs for large industries is very high and can see in Cement Manufacturing Industry very often. It uses for crushing raw material, material grinding with ball mills, material transporting with fuller pumps, and for with large centrifugal fans and with gantry cranes. We can see WRIM in Puttalam cement Plant from 11kW to

1345kW and the operating voltages are 415V for smaller capacity motors and 3.3kV for large capacity motors. For any industry, availability and reliability of a machine is very important. We have experienced considerable startup delays with the conventional starters of WRIM due to its electromechanical nature. Replacing a conventional starter with a VFD is not feasible always, specially when there is no process requirement for variable speeds.

1.2 Motivation:

As conventional starters require a higher number of maintenance routines and time taken to diagnose and rectify if any problem occurs is very high. Therefore finding and alternative starting method for WRIMs with the use of Power Electronics would be great. Basic idea of developing a concept or a power electronics design here is to replace the conventional starter by a Power Electronics Device with a higher duty and reliability.

1.3 Operation of WRIM with a Rotor Resistance Starter:

General practice with WRIMs is to have an external rotor resistance starter and vary the external resistance by steps. Figure 1.1 shows the behavior of starting current and torque development of the rotor with respect to the rotor speed. The advantage of WRIM with external starter over a squirrel cage motor is to have a higher starting torque at a low starting current. [1]

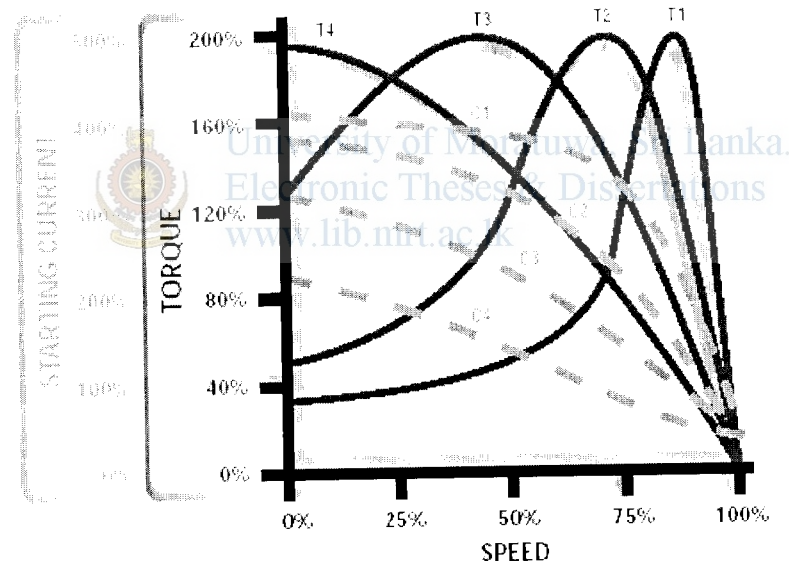


Fig-1.1: Starting Current/Torque vs. Speed of WRIM

1.4 Typical Nameplate data of WRIMs:

For the design and construction of the Power Electronics Starter, it is a must to select a WRIM at a feasible size as an initiative. For that purpose nameplate data collection has done with available motors. The table 1.1 shows below the nameplate data of WRIMs. In addition to the nameplate of a squirrel cage motor, rotor voltage and current are given. These two are the most important parameters, one should know for launching the design of the power electronics starter. For the experimental purposes, an 11kW WRIM has been selected, and all the design, simulations and practical constructions and all the tests have

been done with that 11kW WRIM which is from Crompton Parkinson, a UK motor Manufacturer.

Slip Ring Motor Nameplate Data									
Motor	Voltage (V)	Current (A)	Power (kW)	Frequency (Hz)	Speed (rpm)	Power factor	Insulation Class	Application	Make
Stator	415	40	22	50	735	0.8	F	Over Head Crane-Long Travel Motor	Crompton-Parkinson
Rotor	155	87							
Stator	415	20.7	11	50	735	0.8	F	Over Head Crane-Cross Travel Motor	Crompton-Parkinson
Rotor	95	70							
Stator	415	90.5	53	50	735	0.8	F	Over Head Crane-Holding/Closing Motor	Crompton-Parkinson
Rotor	400	80							
Stator	415	95	53	50	975	0.85	B/F	FK Pump- Raw Material Transport	Siemens
Rotor	220	155							
Stator	3300	76	346	50	975	0.87	F	Fan- Raw Material Transport	Siemens
Rotor	670	320							



Electronic Theses & Dissertations
Table-1.1: Typical Nameplate Data of WRIM
www.lib.mrt.ac.lk

Chapter 2

Conventional Starters for WRIM

As in the case of a squirrel cage rotor induction motor, electric power is fed to the stator winding of the WRIM directly. Required protections could introduce via either a combination of a Molded Current Circuit Breaker (MCCB) and Thermal Overload Relay or Motor Protective Circuit Breaker (MPCB). The rotor winding is normally taken to outside control via a slip ring assembly and carbon brushes. In general rotor winding of a WRIM is in star configuration and the ends of those star connected rotor windings are available at the slip rings for external control.

Generally there are no over current or phase unbalance detection for rotor winding specifically, since any abnormality in the rotor circuit is very much reflective at the stator circuit.

There are several techniques to start up an induction motor. They are Direct on Line (DOL) start, Star-Delta start, starting with a soft starter, use of a Variable Frequency Drive (VFD) and use external rotor starter with WRIMs. Squirrel cage induction motors could draw a starting current of 6~8 times of it's nominal current rating without any power electronics starting and as the motor becomes large, this is applying a very significant stress on the power system, switchgears and electrical power cables. But still with a WRIM, there is a chance to minimize the starting inrush current with a starter connected to its rotor. The advantage available with a WRIM is having a higher starting torque at a lower starting current. This is possible with an external rotor resistance starter, which can vary the rotor resistance step by step using electromechanical methods. Basically there are two types, use of power contactors with electrical timers or electrical contacts with a motorized camshaft. Figure 2.1 shows typical rotor resistance starter power contactors. There are four steps, initially the maximum external resistance will apply to the rotor and as the rotor accelerates, external resistance could reduce step by step. Finally the rotor circuit could short-circuit at slip rings via the final power contactor in the sequence and then the rotor will approach the rated speed.

A time delay can introduce to switchover between adjacent speeds to minimize current variations in the motor. But with this step wise starting technique could generate a mechanical jerk to the load as the speed changes, considerable current peaks at the stator winding. The most considerable disadvantage is the speed at any given external resistance highly depends on the load torque and it is not constant.

This conventional starter consists of a large resistor bank, lot of electrical contacts, lot of rotating parts, transformer oil for resistor cooling and providing insulation, several electrical signals to interlock with the power circuit.

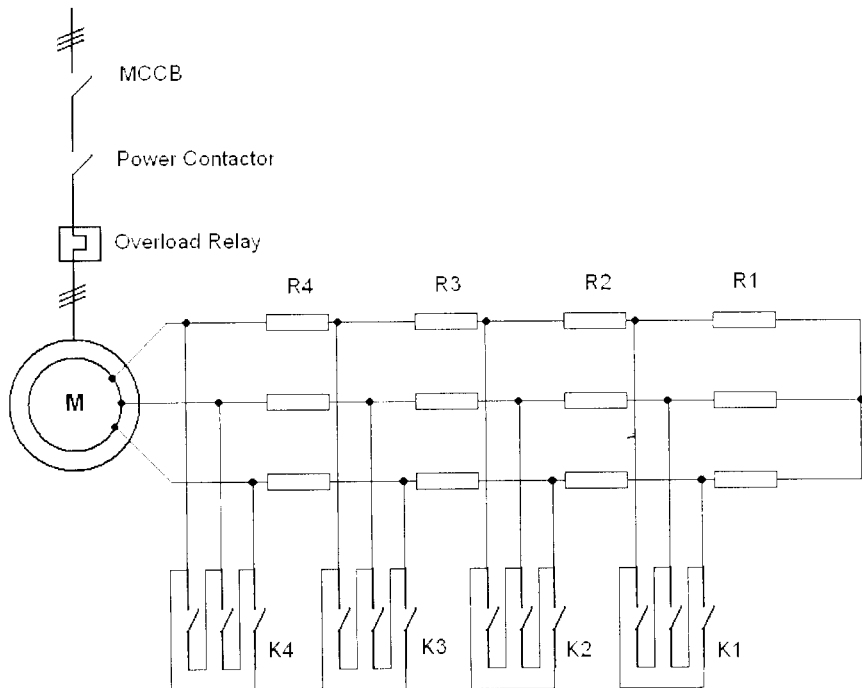


Fig-2.1: Typical External Rotor Resistance Starter of WRIM

Conventional starters are bulky in size and required more maintenance. At every startup detection of starter position is important and there are electrical signals for that, and they are R_{max} position for rotor maximum resistance and R_{min} position for rotor minimum resistance. At the beginning the rotor circuit should be in the R_{max} position and after having a complete successful start, it should be in the R_{min} position for long run operation. Resistor bank has to design to flow initial rotor currents at different steps, and thermal stress on the resistors is high during this period. Transformer oil could use as the cooling media while providing a required insulation. Anyhow there is maximum number of consecutive startups in any given period, and you need to keep time gaps for cooling the external resistor bank for cooling.

WRIM are used for the application, which requires a very high starting torque, like crushers, ball-mills, pumps, large centrifugal fans and hoists. In many occasions, industry experienced lot of startup delays due to the nature of external resistance starter. It needs to position to R_{max} before the startup, all the rotating parts and electrical contacts should be in very healthy condition, after a successful startup rotor starter should come to R_{min} position. At the motor control circuit these signals (R_{max} , R_{min}) need to be evaluated correctly for ensuring the right operation of the motor and the starter. Generally reliability of these rotary-electromechanical parts is low, and user has to take extra care on this rotor circuit in a WRIM.

Replacing WRIM rotor starter with a VFD is possible, but when there is no variable speed requirement in the process, the investment for a VFD as a starter is not so feasible.

Chapter 3

Proposed Power Electronics Starter

A power electronics starter for WRIMs is proposed to overcome the drawbacks of the conventional starter while ensuring and enhancing the performance of the external rotor resistance starter. This is a rotor-based starter, which is having a minimum number of electrical connections, and there are no rotating contacts inside the starter other than the slip ring assembly.

This starter consists of a Power Block to handle the rotor current and a micro-controller based Control Unit for smooth startup or speed control.

3.1 Power Block:

Proposed power block is designed to replace the conventional rotor resistance starter, and basically it contained a three-phase full bridge rectifier unit, transistor chopper stage and a fixed external resistance, which connected to the rotor circuit. The figure 3.1 below is showing the electrical circuit of the proposed power electronics starter for WRIM.

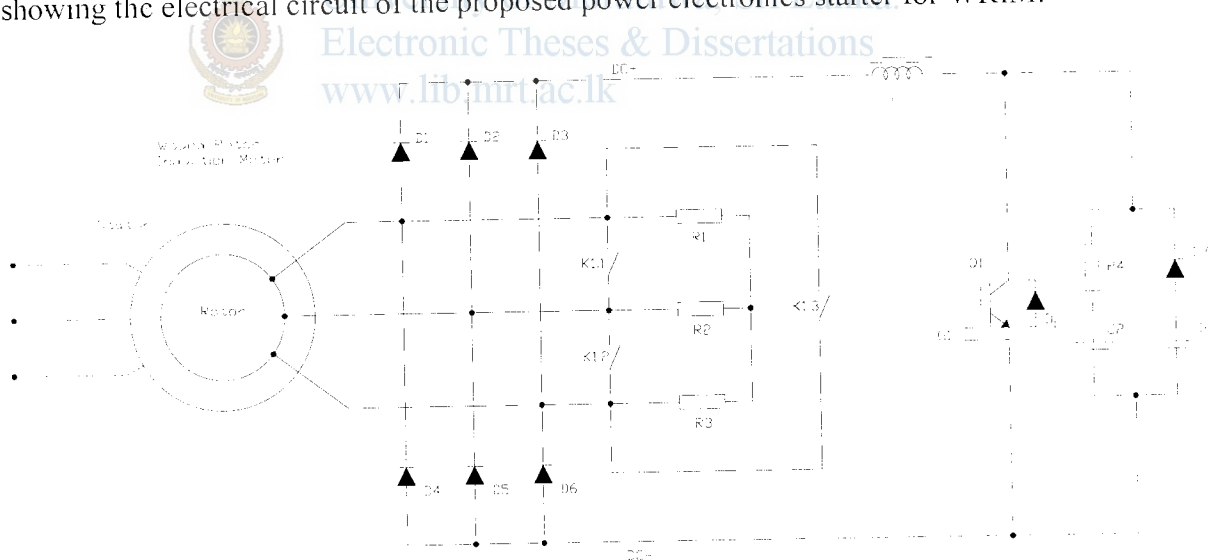


Fig-3.1: Proposed Power Electronics Starter for WRIM

Where:

D1~D6

D_f

R1~R3

- Three-phase full bridge rectifier
- Freewheeling Diode
- External Fixed Resistors

Q1	- IGBT
L	- DC Commutating Choke/ Inductor
R4, C2, C3, D7	- Snubber Circuit
K1	- Bypass Contactor (Optional)

Rotor terminals via slip rings are connected to a three-phase full bridge rectifier and a fixed external resistance (R1~R3). Three-phase rectifier (D1~D6) will convert rotor-induced alternating current into a direct current (DC). The chopper stage connected to the DC link via an inductor (L). This inductor could minimize the switching impacts to the rotor current waveform, and it is known to be the DC-link commutating choke. The chopper contains an Insulated Gate Bipolar Transistor (IGBT) (Q1) as the power switch with a reverse biased diode (D_F) for freewheeling. Snubber circuit will improve the switching characteristics of the IGBT while minimizing the switching stress on the power switch.

Initially the IGBT is fully open and the rotor circuit is loaded entirely by the external resistance only. Sizing of this rotor resistance is very critical and it could determine the starting torque and the initial speed of the rotor without the power electronics starter.

WRIM will accelerate the rotor and reach to the rated speed, as the external rotor resistance becomes zero. In other words rotor reaches to the rated speed once the maximum current flow through the rotor. This power electronics starter can control the current flow through the rotor windings and thereby can control the rotor speed. Current control through the rotor circuit is achieved by the chopper stage, and the IGBT is driven by a Pulse Width Modulation (PWM) scheme to achieve this task. In PWM, it will drive the gate of the IGBT and the duty factor of the transistor can vary from 0~1. As the duty factor is 0, IGBT is fully open and there is no current flow through the chopper. As the duty factor is 1, the IGBT is fully closed and allows to flow maximum possible current through the chopper and consequently through the rotor winding too. Time taken to increase the duty factor of the transistor from 0 to 1 will determine the acceleration of the rotor and the time taken to reach the rated speed. That implies if the duty factor of the transistor is 1, the rotor reaches to the rated speed.

It is obvious that by controlling the duty factor of the transistor, power electronics starter can control the speed of the rotor, by keeping the duty factor at a certain level, rotor speed can be regulated. But the size of eternal resistance will determine the initial speed pf the rotor and could narrow down the range for speed control by the IGBT chopper.

When there is no speed control requirement, once the IGBT received the maximum duty factor i.e.1, there is a facility to bypass the power semiconductors with a power contactor and it will prevent unnecessary loading on power devices and minimize the heating load.

Initially the external resistor bank has to allow the rotor current flow through it and once the power electronics starter controls its duty factor from 0 to 1, the rotor current flow will gradually increase and transfer smoothly and completely from resistor bank to IGBT chopper.

Here the gate driving of the IGBT is achieved by a control unit, which delivers the PWM for the Gate terminal of the transistor.

3.2 Control Unit:

Primary job of the control unit is to drive the gate terminal of the IGBT under a PWM scheme. Control unit provides the facility for programming the base frequency or the pulse frequency for the transistor and can control the duty factor of the IGBT from 0 to 1.

User can increase or decrease the duty factor manually or duty factor increase or decrease can be achieved within a pre-programmed time period automatically, that time period is known as the ramp-up time and ramp-down time respectively.

Central processor for the control unit is a micro-controller, which delivers a hardware PWM scheme and will amplify and process through an IGBT gate driver stage before connecting the gate terminal of the transistor.

In the industry, there are two separate circuits to control the stator and rotor windings of a WRIM, and it is more trouble. The idea of this control unit is not to drive the gate terminal of the IGBT and it can extend to start and stop the stator power supply too. The conceptual schematic of the control unit of the proposed starter is given in the figure 3.2 below.

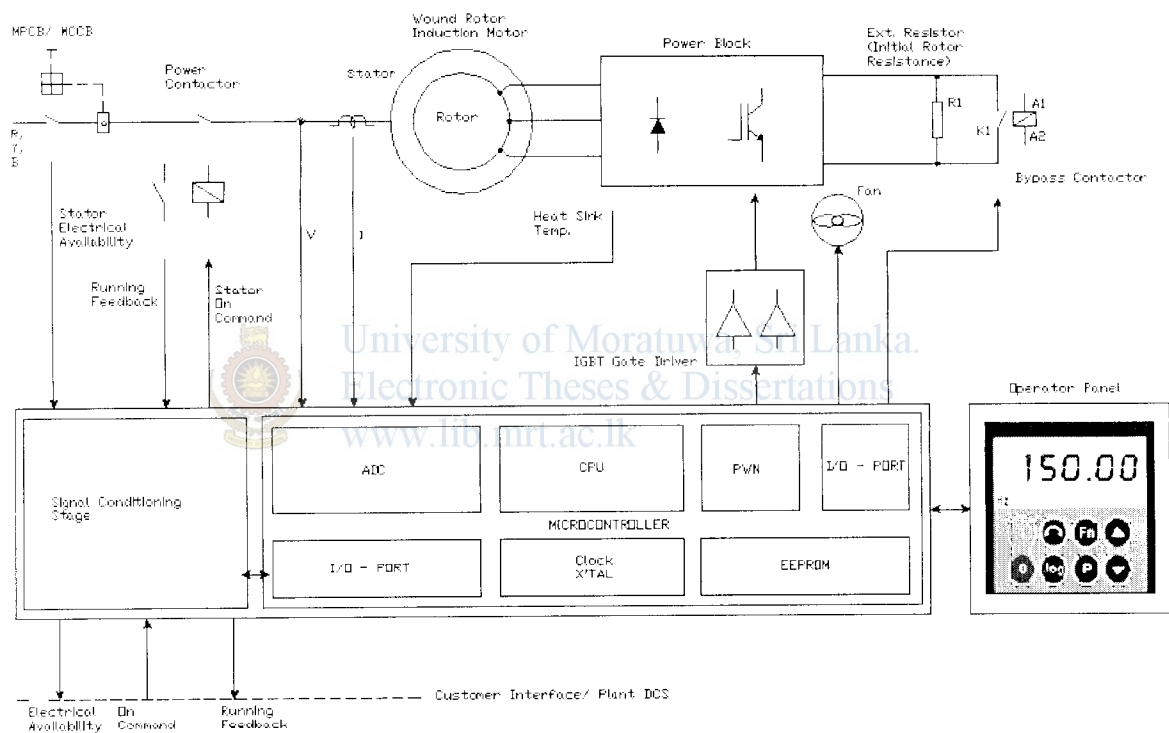


Fig-3.2: Control Unit for Proposed Power Electronics Starter of WRIM

Chapter 4

Identifying Motor Parameters

It is a good engineering practice to investigate the successfullness of the design via simulations before the implementations. In this case also it is more advisable to simulate the design for expected operations via computer tools. For the simulations, the power electronics starter has to model to suit for the selected simulation package. For a successful simulation, identifying the circuit parameters is very important. In this case identifying motor parameters is a must for any kind of simulation. For this project, an 11kW WRIM has been selected by considering the ease of implementation and availability. Typical nameplate data of the selected WRIM for the project is given in the table 4.1 below.

Motor Nameplate Data			
Stator		Rotor	
Voltage	415V	Voltage	95V
Current	20.7A	Current	70A
Power	11kW		
Frequency	50Hz		
Speed	720rpm		
Power factor	0.8		
Insulation class	F		

Table-4.1: Nameplate Data of 11kW WRIM

There are two types to identify the motor parameters, one is the Standard test to identify motor parameters and the other one is to perform the motor identification routines with a VFD.

4.1 Standard Tests:

By using the standard test, motor parameters can be identified as it does with a transformer. Here the No Load Test and the Locked Rotor Test are the two types of tests. Both tests have been carried out as a star and a delta configuration at the stator terminals.

During the No Load Test, Rated voltage will apply to the stator winding and need measure the current flow through the winding and the power consumption of the no load motor. During the Locked Rotor Test you need to clamp the rotor stand still and increase the stator voltage until the rated current flow through the winding. In this case you need to measure stator voltage, which will allow for flowing the rated current and the power consumption of the locked rotor motor. In simple terms, you need to block the rotor; hence the name of this

test implies Blocked Rotor Test. Table 4.2 is given below the measured data for standard tests for the WRIM.

No	Test Type	Motor Configuration	Measurements		
			Voltage	Current	Power
1	No Load Test	Star	690V	3.85A	3.68kW
2	Locked Rotor Test	Star	191V	11.95A	3.16kW
3	No Load Test	Delta	415V	7.78A	4.47kW
4	Locked Rotor Test	Delta	115V	20.7A	3.29kW

Table-4.2: Results of Standard Motor Tests for 11kW WRIM

Figure 4.1 and 4.2 are shown below the No Load Test and the Locked Rotor Test respectively. For the Locked Rotor Test you need to apply a voltage to stator which is lower than the rated value, in this case, a VFD can be used to apply a reduced voltage with a suitable programming.

4.2 No Load Test:

Figure 4.1 shows below, carry out of no load test for the WRIM.

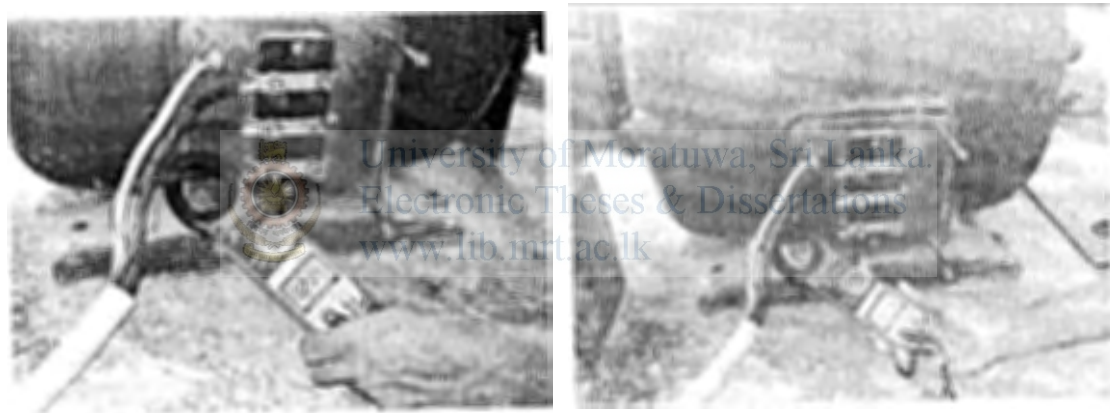


Fig-4.1: Carry out of No-Load-Test for 11kW WRIM

4.3 Locked Rotor Test:

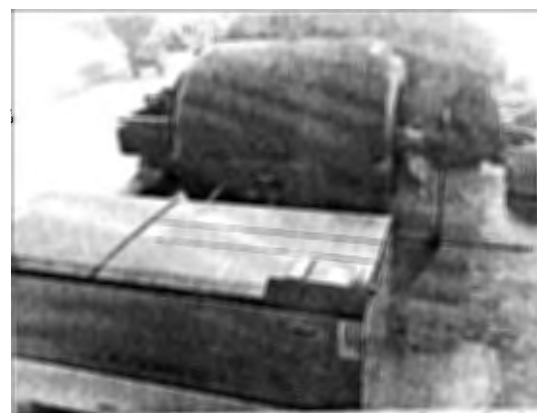


Fig-4.2: Carry out of Locked-Rotor-Test for 11kW WRIM

Figure 4.2 above shows; carry out of the locked rotor test with the WRIM, a VFD is used to control the stator voltage until the rated current flow through the winding.

Identifying motor parameters with standard tests required a manual calculation. With suitable assumptions and measured data, motor parameters can be calculated. [2]

4.4 Identifying Motor Parameters with a VSD:

There is an optional way to find motor parameters by using a VFD. Modern VFDs are having a facility to identify all-important motor parameters and that will improve the operating performance of a motor with a VFD. There is a special routine for this, is known to be the Motor Identification routine. In this case, a Siemens Micromaster VFD has used and it has commissioned with the WRIM (11kW). First, you need to enter the nameplate data what you know at the moment and VFD is having two separate functions for identifying motor parameters and motor characteristics. They are Motor Equivalent Circuit Data and Magnetizing characteristics. [3]

For identifying the motor equivalent circuit data, the VFD will model the motor as follows. Figure 4.3 is showing the modeled motor equivalent circuit by the VFD. [3] In this regard, the VFD will calculate the motor equivalent circuit data like, stator resistance, stator leakage inductance, main inductance, rotor leakage inductance, rotor resistance, cable resistance, cable capacitance etc.

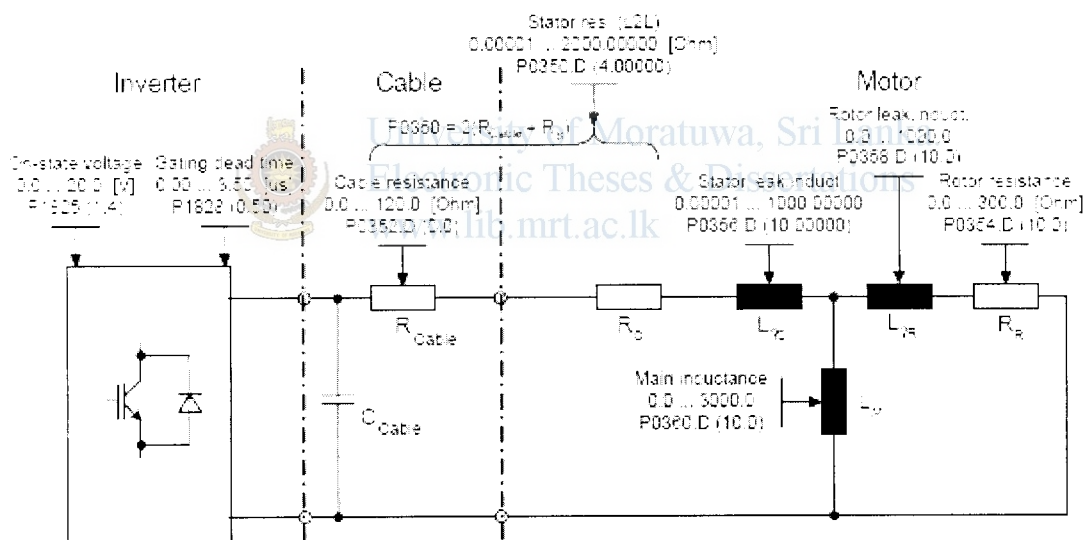


Fig-4.3: Modeling of the Equivalent Circuit Diagram of a Motor by the VSD

After performing motor equivalent data identification test, VFD will proceed for identifying Magnetization characteristics of the motor. During this test the VFD will calculate motor magnetization current, magnetization time, demagnetization time, electrical time constants and other relevant data for motor saturation.

Figure 4.4 given below shows you the identification of magnetization characteristics by the VFD. [3]

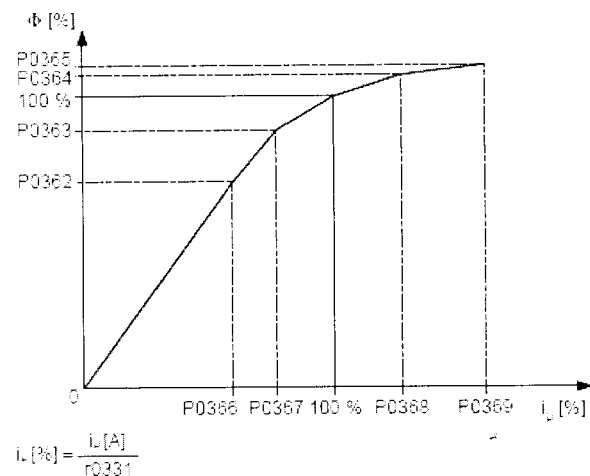


Fig-4.4: Identifying the Magnetizing Characteristics of the Motor

Figure 4.5 below shows an actual figure of a motor-VFD set while performing motor identification routines.



Fig-4.5: Perform Motor Identification Routine of a VSD for 11kW WRIM

To carry out this test, you need to commission the WRIM with the VFD. You can short circuit the rotor circuit at slip rings and the stator winding can be fed via the VFD as in the figure 4.6 below.

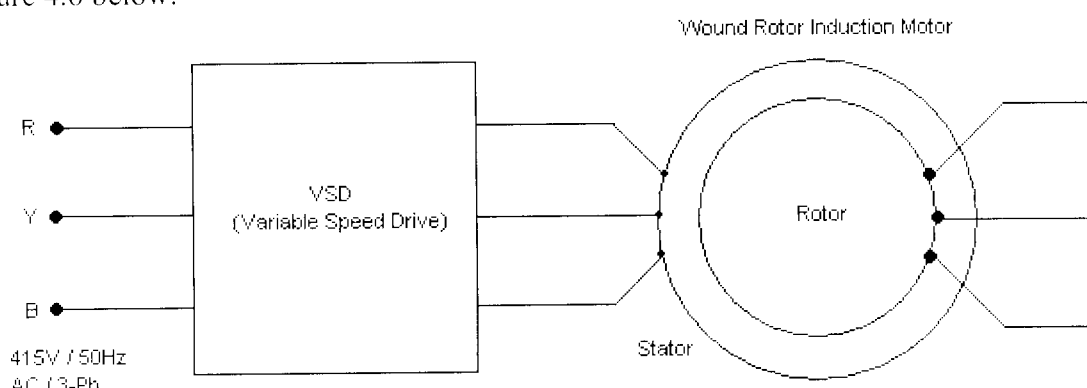


Fig-4.6: Electrical Connections for 11kW WRIM to run with a VSD

Identified motor data with the VFD is given in the table 4.3 below. Parameter numbers as explained in the VFD and its description and measured value are tabulated. [3]

Motor Parameters		Delta Configuration
Parameter No	Description	Measured Value
r0313	Motor pole pairs	4
r0330	Rated motor slip	2%
r0331	Rated magnetization current	9.258A
r0332	Rated power factor	0.8
r0333	Rated motor torque	142.91Nm
P0341	Motor inertia	0.1821kgm ²
P0342	Total/motor inertia ratio	1
P0344	Motor weight	132kg
r0345	Motor start-up time	0.098s
P0346	Magnetization time	0.221s
P0347	Demagnetization time	0.552s
P0350	Stator resistance (line-to-line)	1.1810 Ohm
P0352	Cable resistance	0.0984 Ohm
r0384	Rotor time constant	221ms
r0395	Total stator resistance [%]	5.10%
r0396	Act. rotor resistance	2.67%
r1912	Identified stator resistance U_phase	0.7234
	Identified stator resistance V_phase	0.7155
	Identified stator resistance W_phase	0.7194
r1913	Identified rotor time constant U_phase	85.059
	Identified rotor time constant V_phase	77.854
	Identified rotor time constant W_phase	83.797
r1914	Ident. total leakage inductance U_phase	17.925
	Ident. total leakage inductance V_phase	19.427
	Ident. total leakage inductance W_phase	19.625
r1915	Ident. nom. stator inductance U_phase	96.624
	Ident. nom. stator inductance V_phase	92.383
	Ident. nom. stator inductance W_phase	93.227
r1916	Identified stator inductance 1 U_phase	71.299
	Identified stator inductance 1 V_phase	70.88
	Identified stator inductance 1 W_phase	71.478
r1917	Identified stator inductance 2 U_phase	84.19
	Identified stator inductance 2 V_phase	84.372
	Identified stator inductance 2 W_phase	84.846
r1918	Identified stator inductance 3 U_phase	94.879
	Identified stator inductance 3 V_phase	94.773
	Identified stator inductance 3 W_phase	93.279

Table-4.3: Identified Motor Parameters by the VSD for 11kW WRIM

Chapter 5

Circuit Modeling and Simulation

Simulation is a good practice in the engineering world in prior to the implementation. In this case Matlab Simulink Package has been selected for the simulations. With the identified circuit parameters, the designed circuit as in the figure 3.1 has been modeled in the Simulink by using SimPowerSystems library and with the help of some other demonstrations available in the help-Simulink. [4]

Figure 5.1 below is the modeled circuit with the Matlab-Simulink package. Here the 11kW WRIM is in place with required data, a three phase 415V/ 50Hz power source is feeding the stator, rotor windings are connected to an external resistor in star configuration, and a three phase rectifier module is also connected to the rotor winding parallel to the external resistor. IGBT is in place as the transistor chopper and it is linked to the DC bus via the DC commutating choke. Snubber components are also there for simulation. Two numbers of ideal switches are representing the bypass contactor in actual circuit. A pulse generator, which is having a facility to program the pulse frequency and the duty factor of the square waveform, performs gate drive of the IGBT and an oscilloscope is connected to see the pulse train to the gate terminal of the IGBT.

Three-Phase Asynchronous Machine

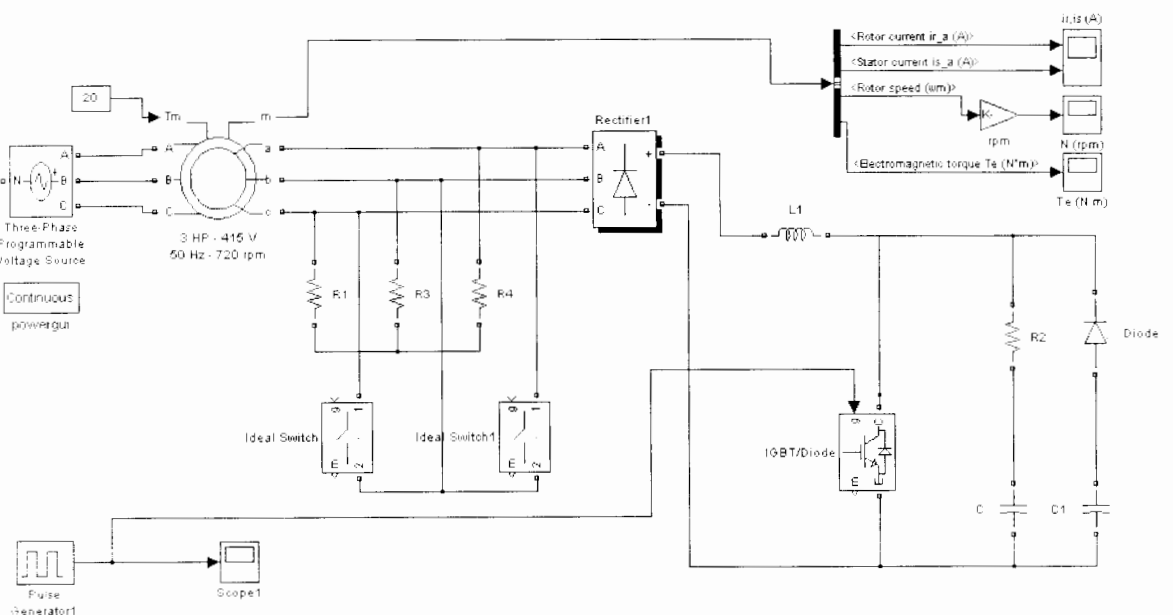


Fig-5.1: Circuit Modeling with Matlab-Simulink

Three separate oscilloscopes are used to observe and trace the behavior of Rotor Current (I_R) and Stator Current (I_S), Speed of the Rotor (N_{rpm}) and the Electromagnetic Torque (T_e) Development of the rotor.

Several numbers of simulations has done for identifying the feasibility of the design, while improving the performance.

5.1 Simulation – Set1:

Circuit modeled as in the figure 5.1 is used for simulation-set1. Here the Pulse frequency is kept as 100Hz constant and varied the duty factor (D) of the IGBT from 1% (min) to 99% (max) manually in step by step. Other circuit values for simulation as follows, $L_1 = 1mH$, Ext Resistance– 33Ohm/ Star Bridge, Snubber - $R_2 = 27\Omega$, $C = 2.2nF$, $C_1 = 0.11\mu F$.

Figure 5.2 shows below the simulation results for Rotor Current (I_R) and Stator Current (I_S) separately. You will see with the duty factor (D), the variations in the current profiles of the rotor and stator.

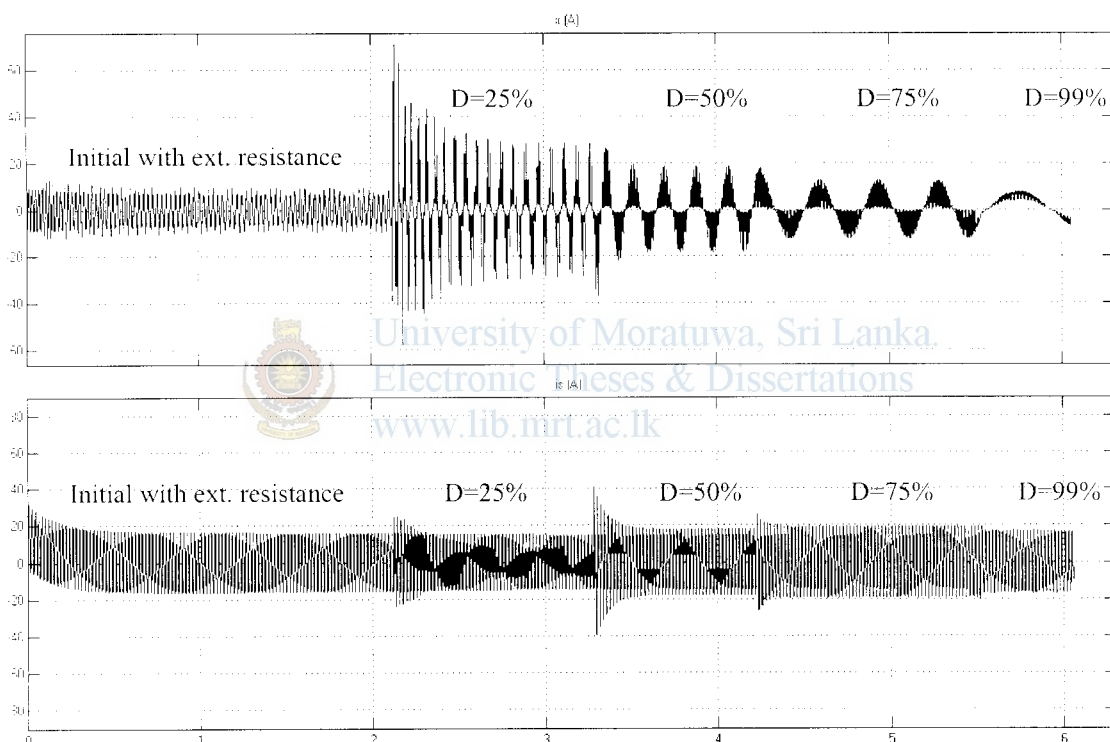


Fig-5.2: I_R -Rotor Current and I_S -Stator Current Vs. Time [Pulse Freq. – 100Hz]

Further, a closer look on the current profiles of the motor give a more clear picture, and can see the impacts due to the rotor and stator current waveforms as in the figure 5.3 below. We can see a clear discontinuation of the rotor current at a pulse frequency of 100Hz and the impacts to the rotor has clearly reflected to the stator winding too. Stator current waveform is also deviating from its original sine wave.

The switching impacts to the rotor should be compensated with the DC commutating choke, and its inductance is important in this regard. After having several simulations, it has proven with a higher value of inductance (Ex: $L=200mH$) this switching impacts could be minimized at this pulse frequency. But a 200mH inductor is a very bulky component

and its resistance could add extra resistance to the rotor winding and the power loss is also high. Feasible level for the inductance is 1mH to 10mH range and as it closer to 1mH very small in size. The idea is to keep the inductance at 1mH and increase the pulse frequency and see the impacts to the rotor and stator current profiles.

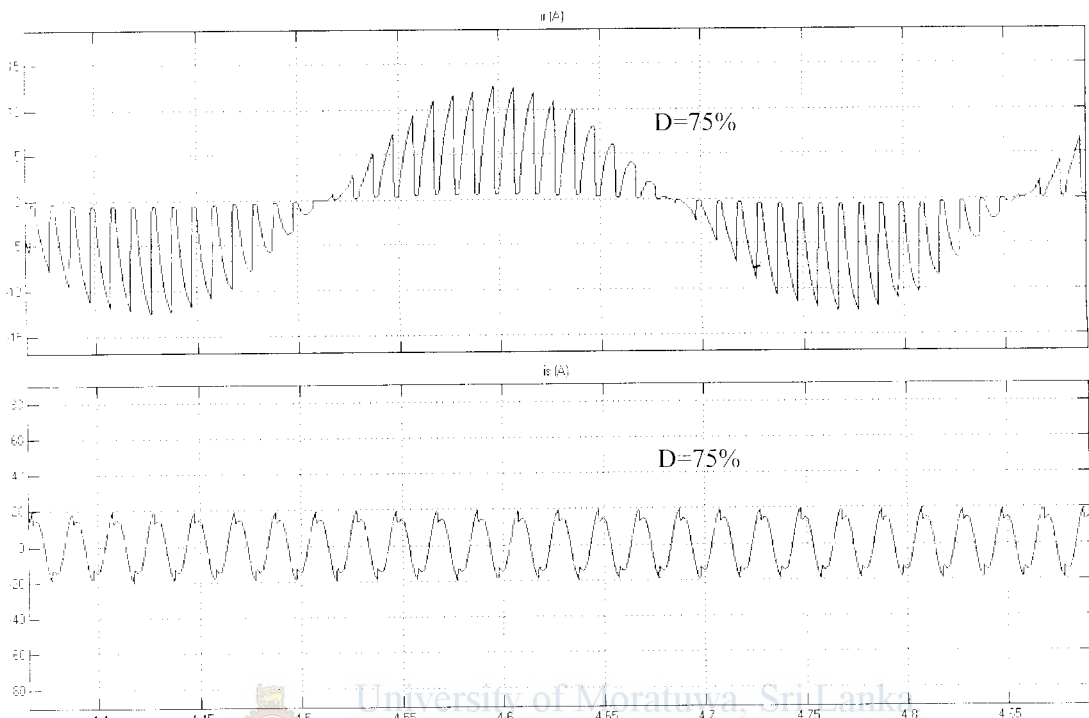


Fig-5.3: Closer look on Current Profiles of Rotor and Stator at $D=75\%$ [Pulse Freq. – 100Hz]

The important thing is to analyze whether the rotor can develop its speed with an increased duty factor of the IGBT. Yes, it can do. As the duty factor of the IGBT increases, rotor speed will develop. In this case simulations are completed for different duty factors like, 1% (min- to see the initial speed development with external resistance), 25%, 50%, 75% and 99%. The speed development of rotor vs. Time at different duty factors of the IGBT is given in the figure 5.4 below.

Another important parameter is the torque development of the rotor as the power electronics starter does the motor starting job. You can see the electromagnetic torque development at different duties of the IGBT in figure 5.5 below.

For the simulations, the rated torque of the motor is taken as 20Nm. Initial torque development is entirely decided by the size of the external resistance and it is a 33Ohm star bridge in this case. At lower duty factors of the transistor chopper, the torque variations are high, and as the duty will closer to 100%, torque fluctuations are very small. The torque fluctuations could compensate by the inertia of the rotor and the inertia of the load when it is connected to a load.

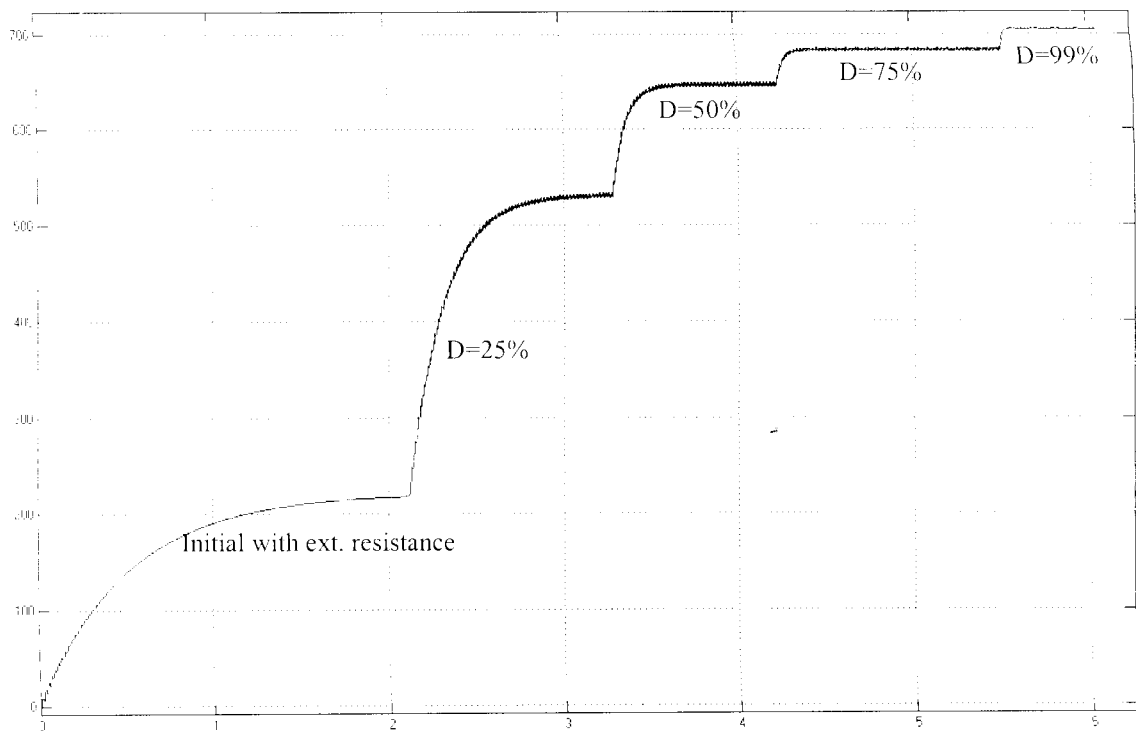


Fig-5.4: Rotor Speed Development with Different Duty Factors [Pulse Freq. – 100Hz]

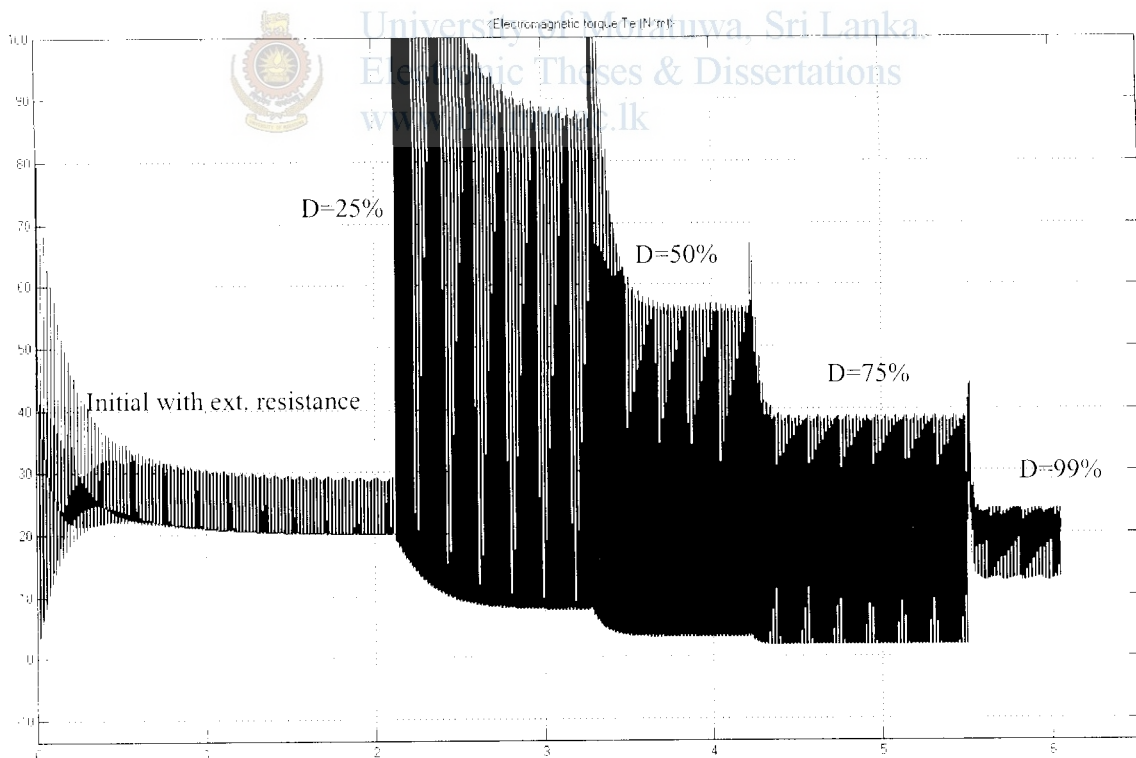


Fig-5.5: Electromagnetic Torque Development with Different Duty Factors [Pulse Freq. – 100Hz]

5.2 Simulation – Set2:

It is clear that to minimize switching impacts, increasing the size of the inductor is not the choice. The most suitable way to minimize the switching impacts is to increase the pulse frequency and see the improvement. For this task, it is required to simulate the model with different pulse frequencies.

In this case, 1 kHz has been selected as the pulse frequency, and all other circuit parameters are kept as constants. Here too, the duty factor of the transistor varies from 1% initially, then 25%, 50%, 75%, and 99% finally. Figure 5.6 below shows you the rotor and stator current profiles I_R and I_S respectively. See the improvement. Discontinuation of rotor current waveform vanishes with higher pulse frequencies, but even with 1 kHz deviation from original sine wave is very high and need to look for further.

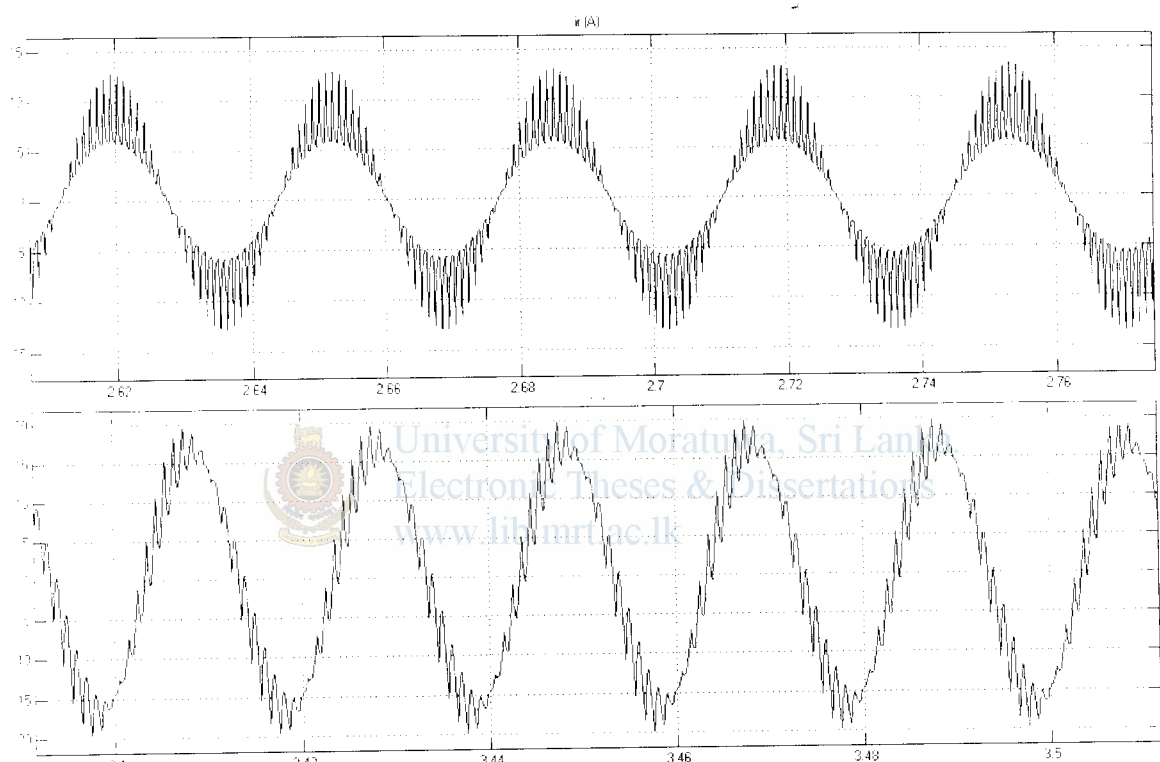


Fig-5.6: Closer look on Current Profiles of Rotor and Stator [Pulse Freq. – 1kHz]

Next selection for the pulse frequency is 5 kHz. Change the pulse frequency of the pulse generator into 5 kHz and while keeping all other parameters constantly, the simulation has run. This time, the rotor and stator waveforms are closer to its original sine wave, and impacts due to switching has minimized. Figure 5.7 gives a closer look on rotor and stator current profiles of WRIM with power electronics starter at a pulse frequency of 5 kHz.

It is clear that, by increasing the pulse frequency of the IGBT, performance of the starter can enhance and the switching impacts to current waveforms can minimize. Final simulation on pulse frequency is to select 10 kHz, and see the results. It is giving a very smooth sine wave for current profiles even with the switching of IGBT and it is appreciable. Therefore, our choice of pulse frequency for the practical implementation is 10 kHz and the size of the inductor is 1mH. Figure 5.8 shows the current profiles at a pulse

frequency of 10 kHz. There we can see a clear improvement on the current profiles of the rotor and stator as the pulse frequency increases.

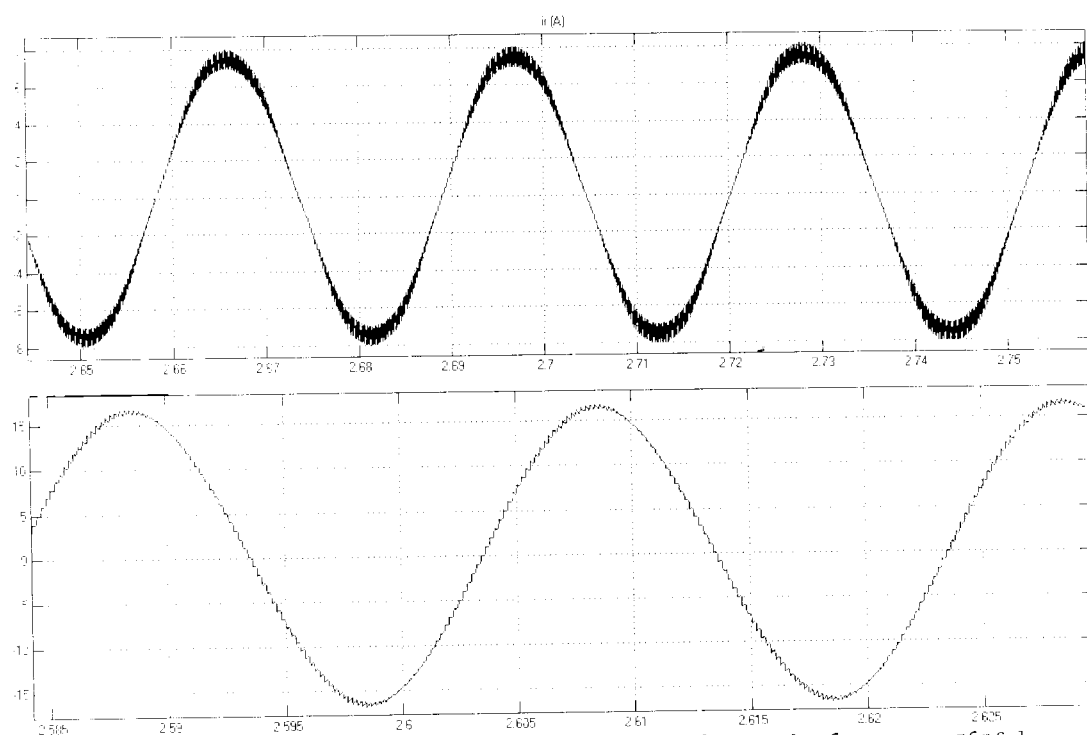


Fig-5.7: Closer look on Current Profiles of Rotor and Stator [Pulse Freq. – 5kHz]

University of Moratuwa, Sri Lanka.



Electronic Theses & Dissertations

www.lib.mrt.ac.lk

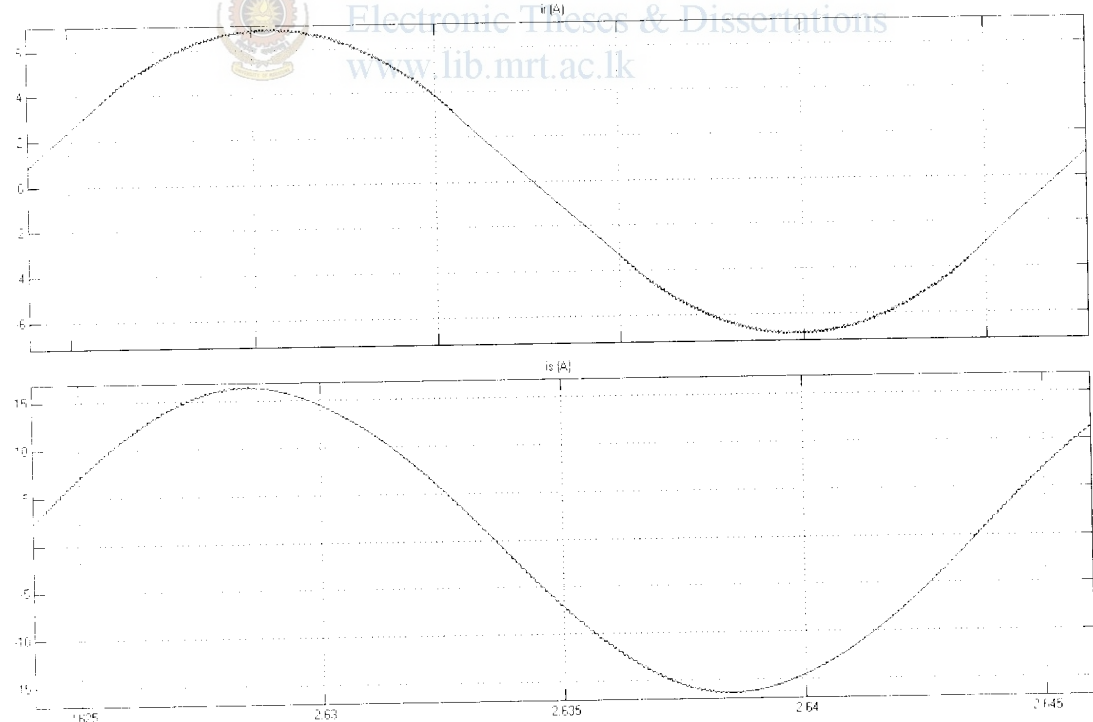


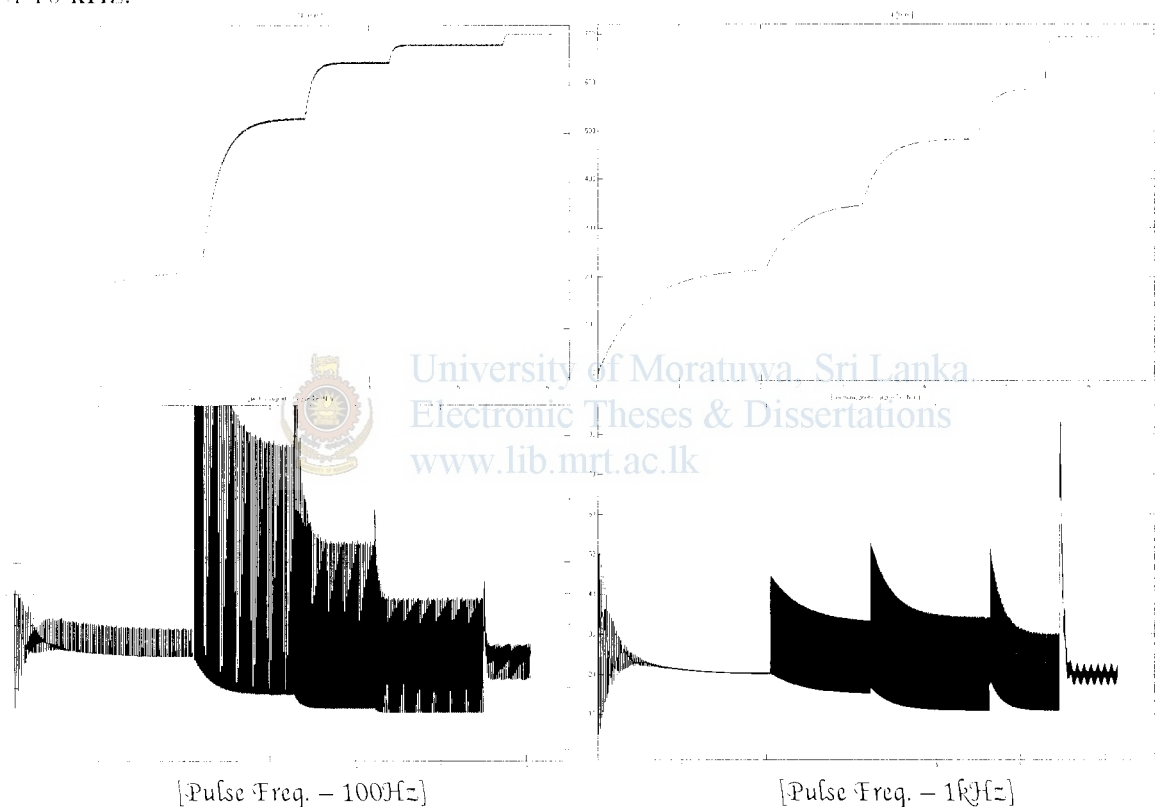
Fig-5.8: Closer look on Current Profiles of Rotor and Stator [Pulse Freq. – 10kHz]

Base pulse frequency of 10 kHz or even higher is not a great deal with today's microcontrollers. As the pulse frequency increases the only concern is the derating of power handling of the semiconductors, in this case it is an IGBT.

5.3 Simulation – Set3:

Simulation set compares and contrasts the effects to rotor speed development and electromagnetic torque development of rotor at different pulse frequencies. Rotor speed fluctuations become negligible at higher pulse frequencies. Electromagnetic torque fluctuations are also become smaller at higher pulse frequencies. Simulations have done by giving a duty factor manually to IGBT.

Figure 5.9 gives a graphical view on the rotor speed development and electromagnetic torque fluctuations with different pulse frequencies. In this case 100Hz and 1 kHz have been selected. Obviously, the motor will have improved characteristics at a pulse frequency of 10 kHz.



[Pulse Freq. – 100Hz] [Pulse Freq. – 1kHz]

Fig-5.9: Speed and Torque Development of Rotor at 100Hz and 1kHz

It is good to simulate and analyze the initial rotor and stator current waveforms. During this time the power switch is in offline and only the external resistance is connected. With externally connected resistance, there is no deviation from the original sine wave of the current profiles, and it shows very clearly in the figure 5.10 below.

Similarly, once the starter completed the starting of the motor or the rotor reaches to the rated speed, you can short-circuit the rotor windings at the slip rings as in the case of a conventional rotor resistance starter for WRIM. Figure 5.11 shows the rotor and stator current profiles at the rated speed. The proposed power electronics starter is having a

bypass contactor to bypass the power semiconductors, when the application doesn't require a variable speed operation for long run.

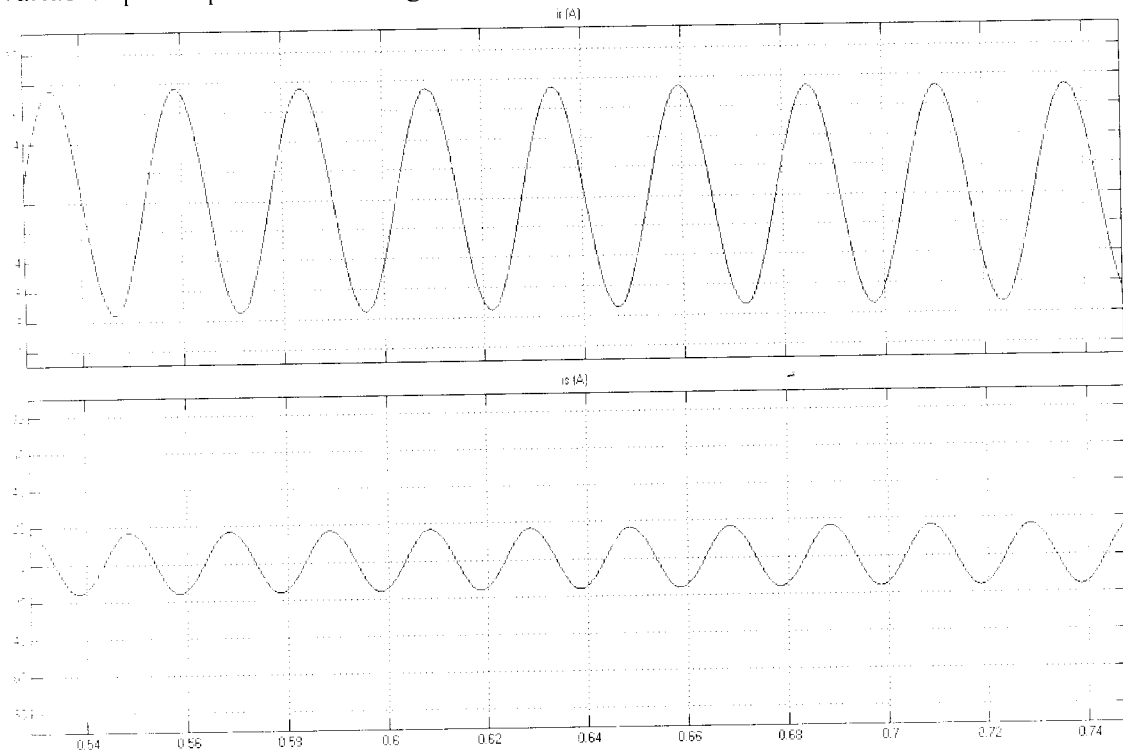


Fig-5.10: Initial Current Profiles of Motor – Duty of $IGBT = 0$ and with connected Ext. Resistor
University of Moratuwa, Sri Lanka.

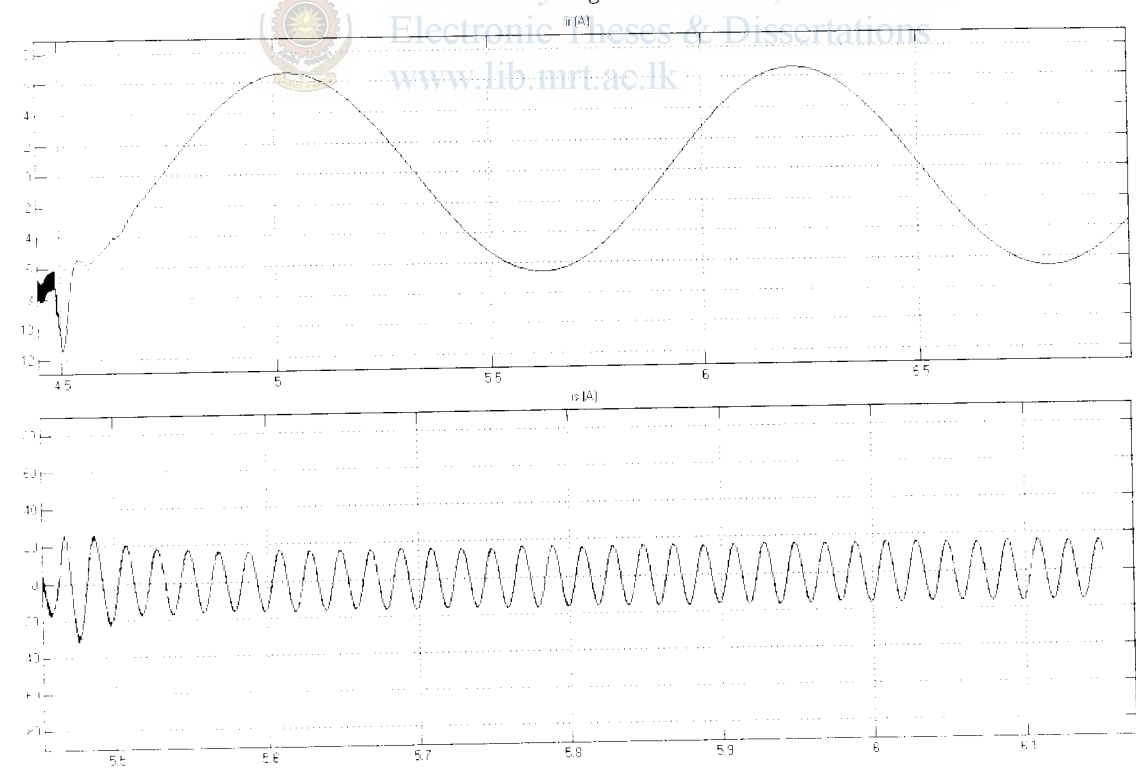
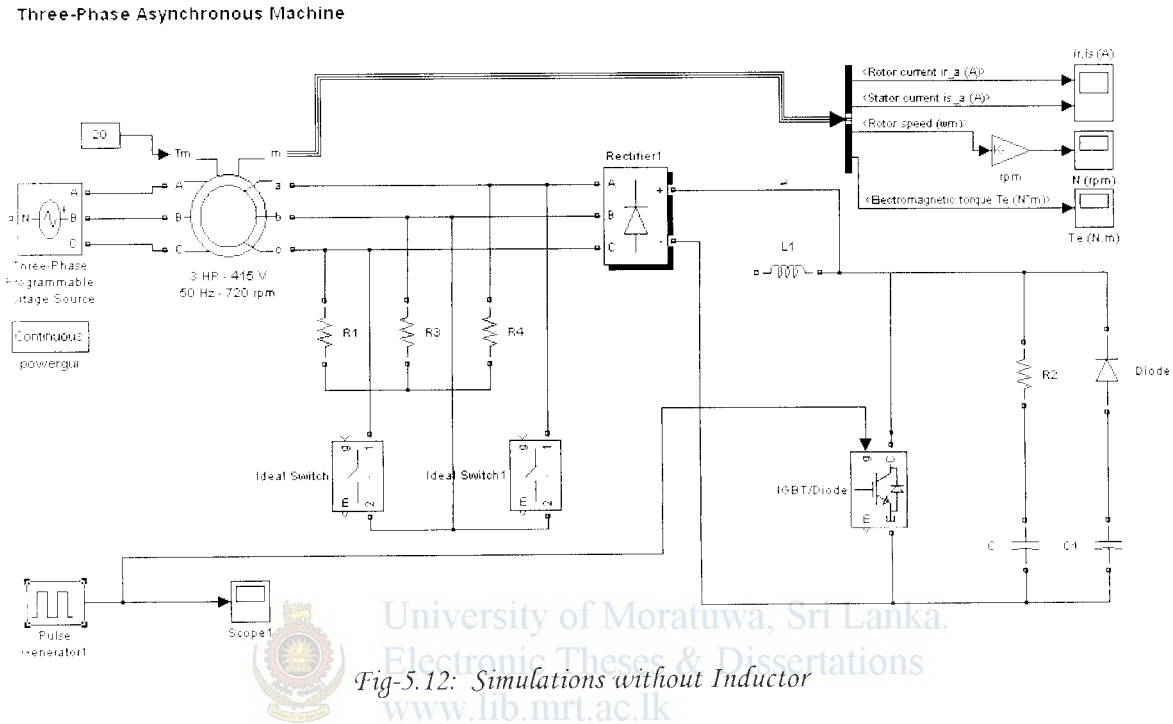


Fig-5.11: Final Current Profiles of Motor – Duty of $IGBT = 1$

5.4 Simulation – Set4:

Simulations below show the importance of some electric components available in the design of proposed power electronics starter. Let's see the impacts to the rotor and stator current without the DC link commutating choke or the inductor by keeping all other components as they are. Pulse frequency is 1 kHz and the duty factor of the transistor is 50% for this simulation. Figure 5.12 shows below the modeled circuit with Simulink package.



It is clear that without the inductor, the switching stress on the rotor and stator current profiles are very high irrespective to the pulse frequency. Anyhow the impacts are very significant at lower pulse frequencies. Without the inductor in the DC link, again a discontinuation started in the rotor current profile and stator current profile is also disturbed heavily. Further the impacts to the electromagnetic torque development are also considerable. Figure 5.13 below shows the rotor and stator current profiles without the inductor at a pulse frequency of 1 kHz.

Actually, there is no commutation to the switching impacts generated by the IGBT without the inductor and hence the name implies to this inductor as the DC Link Commutating Choke.

Next simulation shows to have an external resistance connected to the rotor circuit. Modeled circuit in the Simulink package without an external resistance is shown below in the figure 5.14. When there is no external resistance connected to the rotor, it will open circuit for a very short time during the switching. Opening the rotor circuit will stop rotor current flow for a while and there would be severe impacts to the original current profiles of the rotor and stator, and this is having a significant impact to the electromagnetic torque development of the rotor too. Figure 5.15 gives a clear picture on the behavior of rotor and stator current profiles.

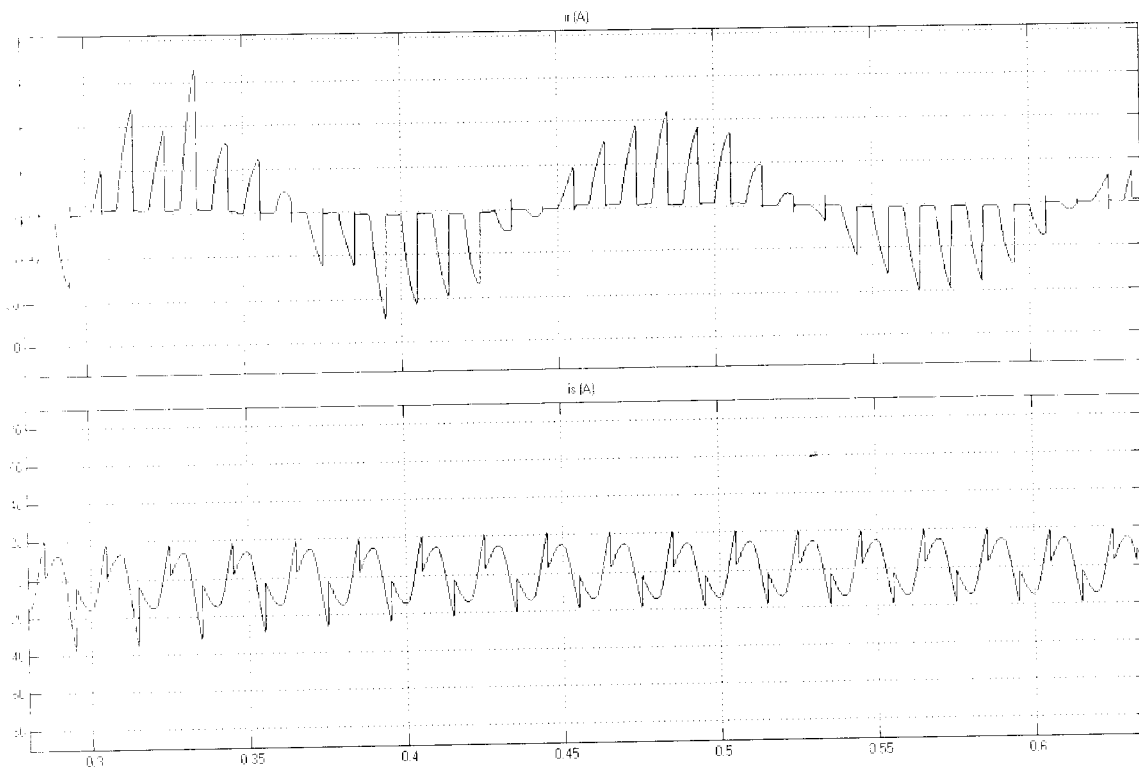


Fig-5.13: Rotor and Stator Current Profiles without Inductor

Three-Phase Asynchronous Machine

University of Moratuwa, Sri Lanka
Electronic Theses & Dissertations
www.lib.mrt.ac.lk

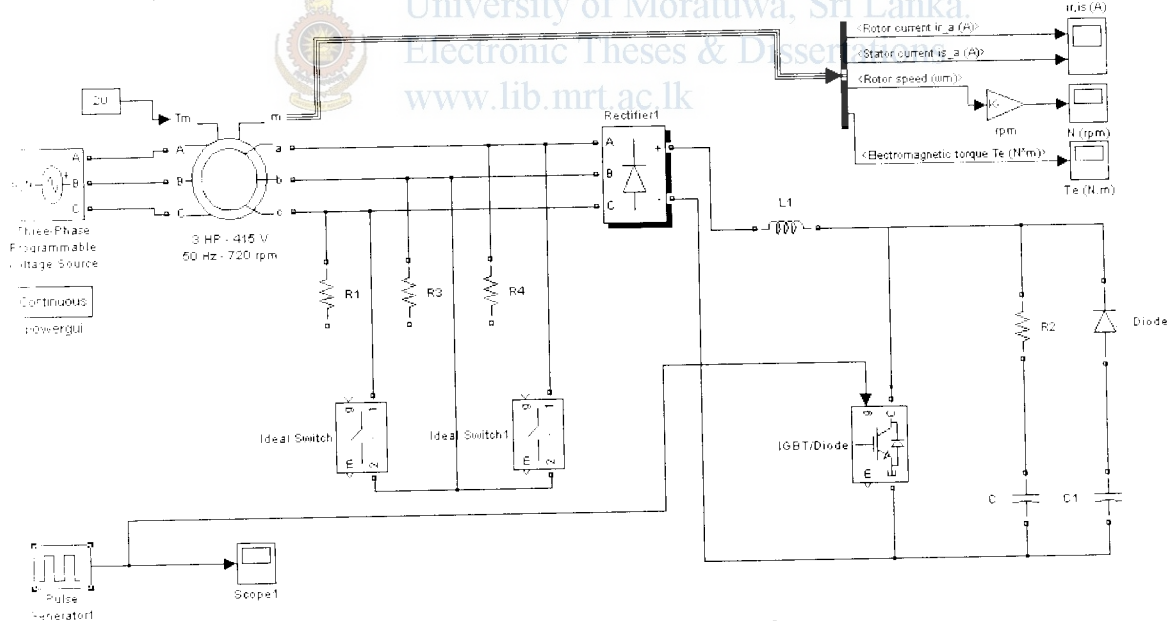


Fig-5.14: Simulations without External Resistor

When there is no external resistance, rotor current fluctuations are severe and deviating very much from the sine wave. There we can see fast rising and decaying and the peak-to-peak variation is very high. Further the stator current profile is also distorted heavily, when the external resistor is not in place.

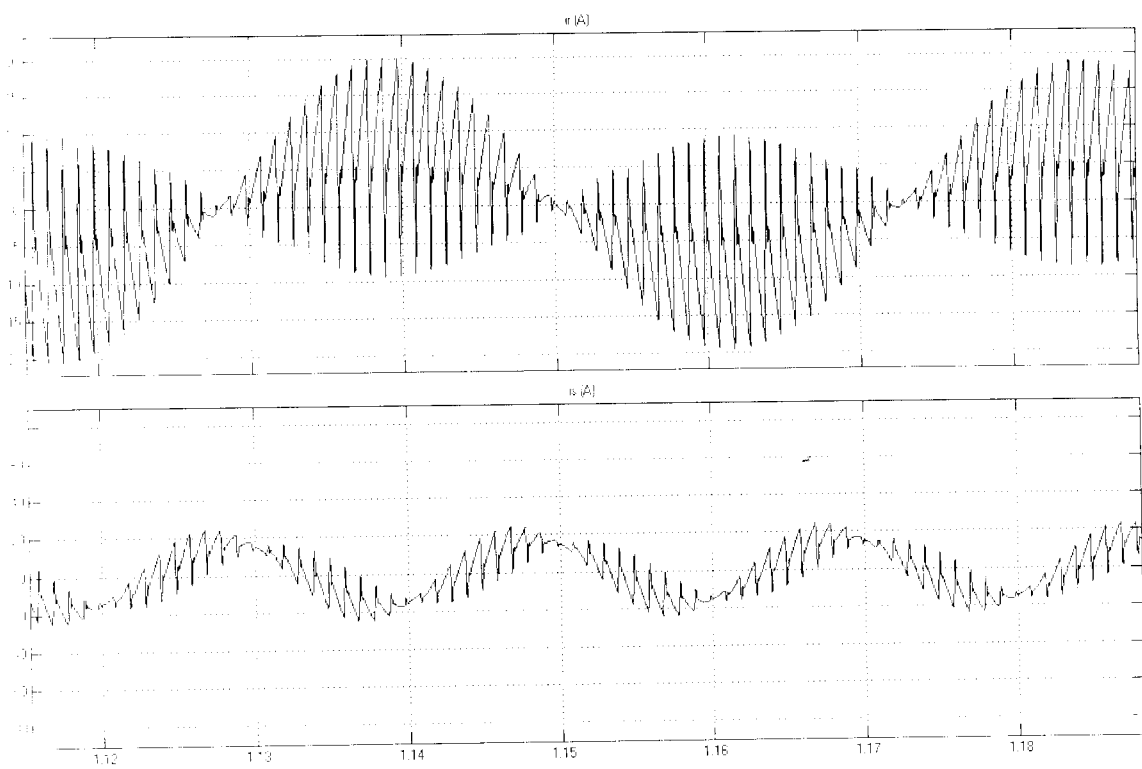


Fig-5.15: Rotor and Stator Current Profiles without External Resistor



University of Moratuwa, Sri Lanka.
Electronic Theses & Dissertations
www.lib.mrt.ac.lk

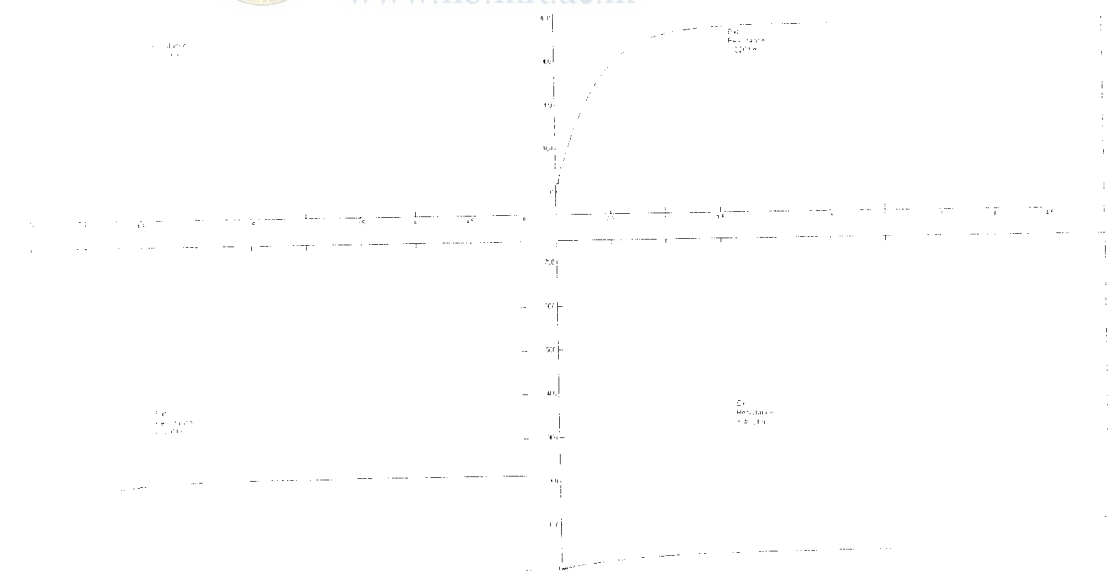


Fig-5.16: Comparison of Rotor Speed Development vs. Time with Different External Resistances

It is obvious, that an external resistor is essential for optimum operation of the power electronics starter. But the sizing of this resistance is very tactful. Starting torque of the rotor will determine by this external resistance, but as the external resistance becomes smaller, initial rotor speed will be very high. Finally the range for speed control by the power electronics starter will be narrow.

As per the simulations, with a 33Ohm star bridge of external resistance, initial speed of the rotor will be 200rpm approximately. This is clearly visible in the figure 5.16 above, and it is showing initial speeds of rotor with different external resistances. As the resistance becomes lower, the initial speed becomes higher and finally the retaining range for speed control is narrow and vice versa.

Another important consideration with initial resistance is the starting torque of the motor. As the external resistance becomes lower, the starting torque would be higher. This selection should be entirely done base on the load or the application. Simulations has been carried out for 33Ohm star-configured external resistance with the rotor circuit and it could deliver an average starting torque which is slightly higher than the rated motor torque, i.e. 20Nm. There is a maximum limit for increasing the size of resistance, since the resistance becomes higher and higher, starting torque will be lowered.

Figure 5.17 shows below a comparison of electromagnetic torque development of rotor vs. time with different external resistors.



Fig-5.17: Comparison of Torque Development of Rotor vs. Time with Different External Resistances

5.5 Simulation – Set5:

In practical life, when there is no speed control requirement, if the power electronics starter is using as a starter of the WRIM, the duty factor of the IGBT has to increase from 0 to 1 gradually. The time period taken to increase the duty from 0 to 1 should be programmable.

As the duty varies from 0 to 1, the rotor speed is also increasing from initial speed (with external resistance only) to the rated value, and time taken to accelerate up to the rated speed is known as the Ramp-up time very commonly.

For this kind of simulation, we have to modify the pulse generating part for the IGBT slightly. Modified schematic in Simulink is shown below in the figure 5.18. the block of repeating sequence is used as the base pulse frequency generator, the block of Ramp is pre programmable to a suitable ramp-up time and relational operator is comparing the above two signals and generating a PWM waveform for IGBT. This is the gate signal, which varies the duty factor from 0 to 1 within a given ramp-up time.

Three-Phase Asynchronous Machine

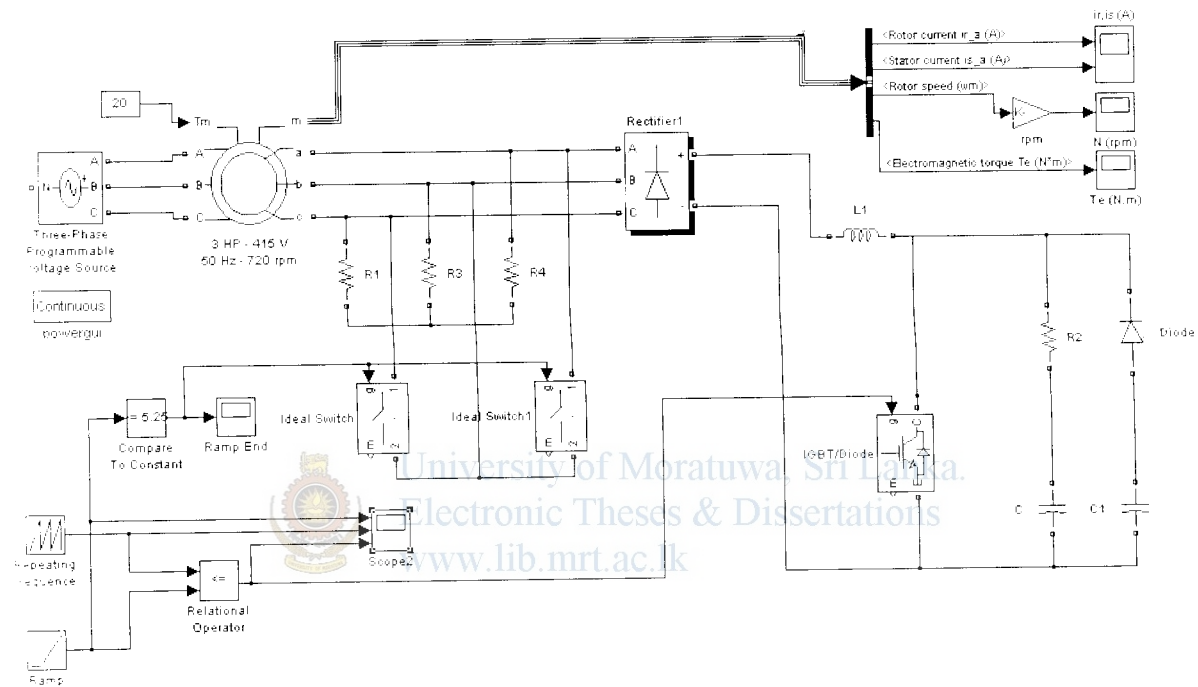
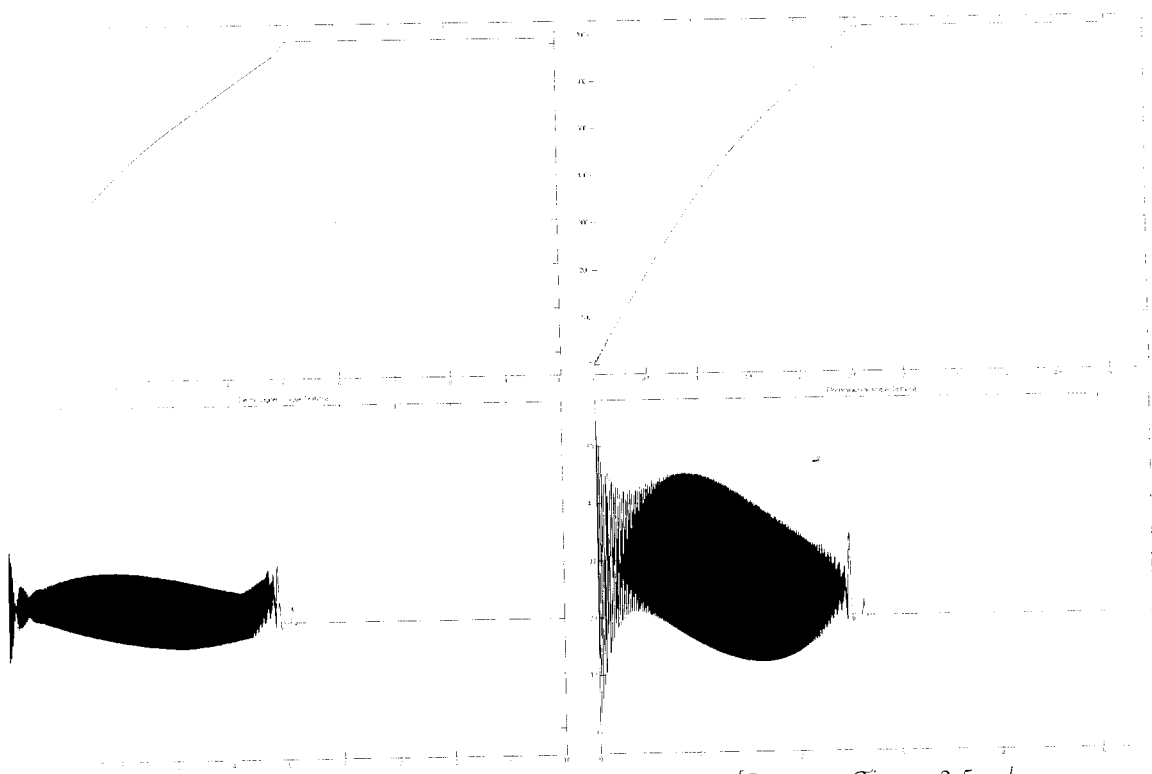


Fig-5.18: Modeled Power Electronics Starter in Simulink for Programmable Ramp Start

Figure 5.19 below shows a result of simulations at different ramp-up times. It is showing speed and electromagnetic torque development of rotor of WRIM at a ramp-up time of 5sec and 2.5sec respectively.

The above curves are derived from the Simulink simulations. But in the real world, ramp-up time is determined by the load inertia. We can't request a very low ramp-up times when there is a large inertial load. For fast ramp-ups, stator needs more currents during the acceleration time, and rotor is also following the stator.

As the figure 5.19 shows below, fluctuations of the electromagnetic torque development of the rotor is also high during a fast ramp-up.

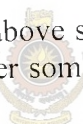


[Ramp-up Time = 5sec]

[Ramp-up Time = 2.5sec]

Fig-5.19: Comparison-Rotor Speed and Torque Development at Different Ramp-up Times

Set of simulations as above shows the feasibility of the proposed power electronics starter for WRIMs, and further some simulations emphasized the duty of certain components and its importance.



Chapter 6

Selection of Power Semiconductors and Hardware Construction

When it's come to the hardware construction of the power electronics starter, the whole starter can be categorized into two separate units called the Power Block and the Control Unit. Mainly the power unit will handle the power part and it will contain power semiconductors, external resistors, DC link components, snubber circuits and a bypass contactor. Control unit is a microcontroller-based unit, which is dealing with TTL level signals, further a gate driver stage is to couple PWM control signal to the power transistor, and in this case it is the IGBT.

6.1 Power Block:

Power block is the physical replacement of the rotor resistor starter of a conventional WRIM. A three-phase rectifier block and an IGBT are the power semiconductors available in the power block. In addition to that a DC link commutating choke, start configure external resistors, Snubber components are available. The figure 6.1 below shows an actual photo of a power block of rotor-based starter for 11kW WRIM.

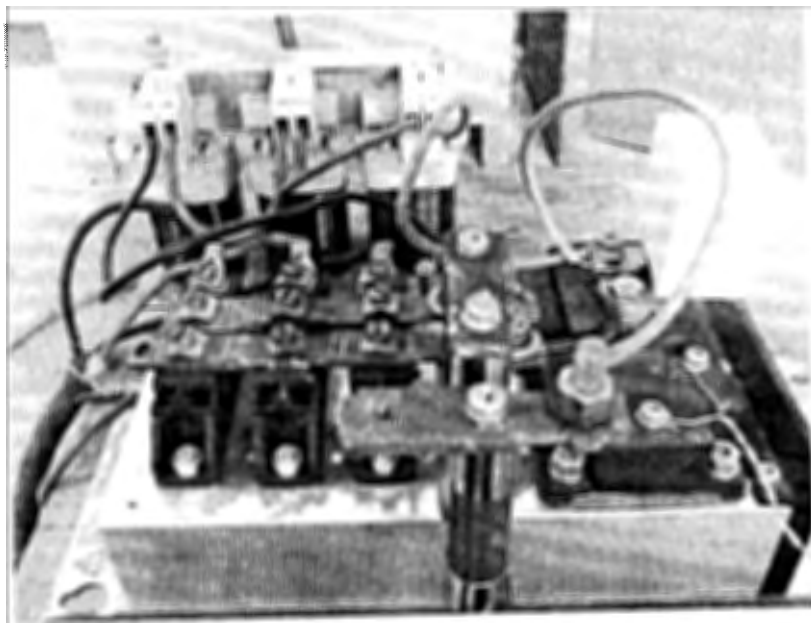


Fig-6.1: Actual Figure of a Power Block of Rotor Based Starter for 11kW WRIM

6.2 Three Phase Rectifier:

Three Phase Rectifier is one of the main power semiconductors available in the power electronics starter. It contains six number of power diodes. For the practical construction, MDD 95-16N1B from IXYS Semiconductors has selected. Two diodes are integrated in one module to form a half bridge as in the figure 6.2 below. Selection of a rectifier is entirely based on the rotor nameplate data of the WRIM, which is connected to the power electronics starter. Here the Forward Current and Peak Inverse Voltage of the diode module are very important parameters for the selection.

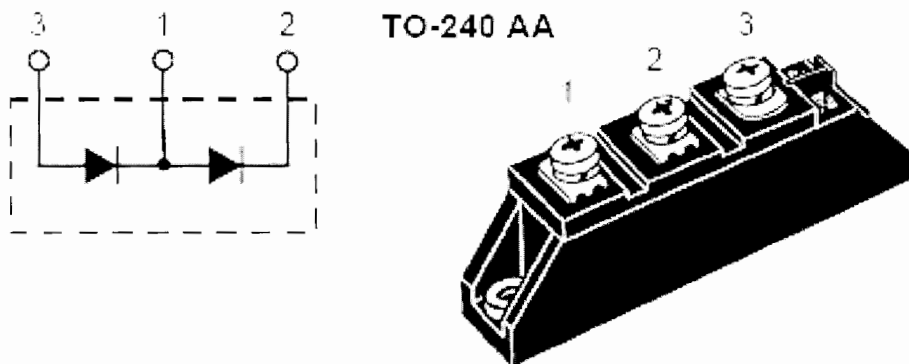


Fig-6.2: Schematic and Actual Figure of a Diode Module – Half Bridge

6.3 Maximum Ratings and Characteristics of Diode Module (MDD 95-16N1B):

Maximum ratings and characteristics of the selected diode module are given below in the table 6.1. [5] Rotor Rated Current is 70A and Rotor Voltage is 95V_{dc} of the selected 11kW WRIM for the experiment. Obviously, the selected diode module is having higher ratings and a higher safety factor for the experimental purposes.

Symbol	Test Conditions	Maximum ratings	
I _{FRMS}	T _{VJ} = T _{VJM}	180	A
I _{FAVM}	T _C = 105 ⁰ C; 180 ⁰ sine	120	A
I _{ESM}	T _{VJ} = 45 ⁰ C; V _R = 0	2800	A
	t = 10 ms (50Hz), sine	3300	A
	T _{VJ} = T _{VJM}	2500	A
	V _R = 0	2750	A
V _{RSM}		1700	V
V _{RRM}		1600	V
$\int f dt$	T _{VJ} = 45 ⁰ C; V _R = 0	39200	A ² s
	t = 10 ms (50Hz), sine	45000	A ² s
	T _{VJ} = T _{VJM}	31200	A ² s
	V _R = 0	31300	A ² s
T _{VJ}		-40...+150	⁰ C
T _{VJM}		150	⁰ C
T _{sig}		-40...+125	⁰ C
V _{ISOL}	50/60Hz, RMS	t = 1 min	3000 V~
	I _{ISOL} ≤ 1 mA	t = 1 s	3600 V~

M _d	Mounting torque (M5)	2.5-4/22-35 Nm/lb.in.
	Terminal connection torque (M5)	2.5-4/22-35 Nm/lb.in.
Weight	Typical including screws	90 g

Table-6.1: Ratings of Diode Module

6.4 Calculation of Forward Current and Peak Inverse Voltage of Three-Phase Rectifier:

For the calculation of above data, it is required to investigate the electrical circuit of the proposed power electronics starter in detail as below. Here the rotor is represented by a three-phase voltage source as in the figure below.

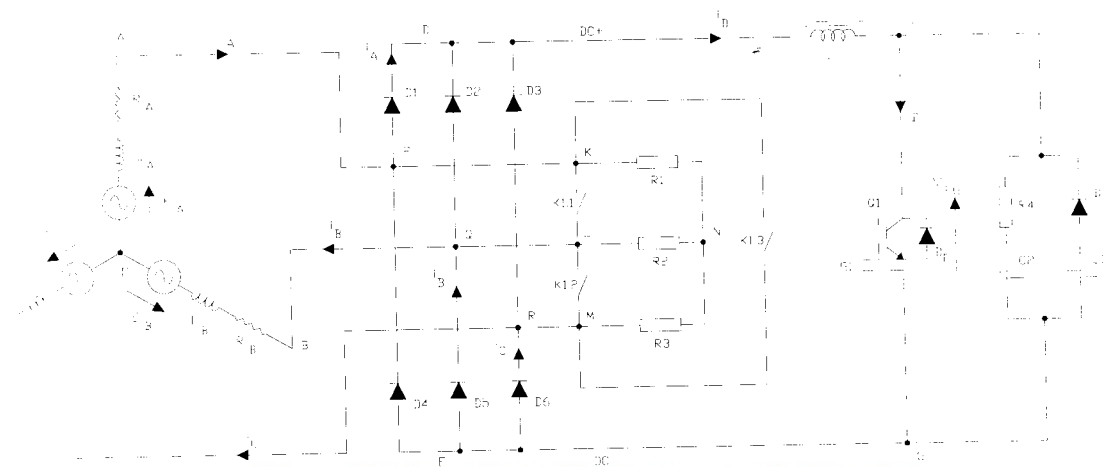


Fig-6.3: Electrical Circuit of the Power Electronics Starter for WRIM

For these calculations, it is needed to refer the nameplate data of the selected motor for the experiment.

$$\text{Rotor Phase Voltage, } E_A = 95V$$

$$\text{Rotor Phase Current, } i_A = 70A$$

Maximum forward current flow through any diode is equal to the maximum rotor current, by assuming motor is not exceeded the rated conditions,

$$\text{Forward Current Rating of the Diode, } i_D = 70A \quad [1]$$

The peak inverse voltage appearing across the diode is the maximum value of the line voltage. [6]

$$\text{Peak Inverse Voltage of the Diode, } V_{PIV} = \sqrt{3} \times 95V = 164.5V \quad [2]$$

Above equations [1] and [2] are showing the rated conditions for the diode, but is a good practice to keep a safety factor for reliable operation. As the safety factor increases the cost for semiconductors will increase and need to find an optimum point based on the experience. Generally a safety factor is applicable.

6.5 Calculation of Collector Current and Collector-Emitter Voltage of IGBT:

The mean value of the load voltage of a three-phase bridge rectifier is as follows. [12]

$$RMS\text{ Voltage of DC Link, } V_{mean} = \frac{3}{\Pi} \times V_{line[\max]} = 90.7V \quad [3]$$

With this, the collector-emitter voltage of the IGBT can be determined.

Maximum current flow through the DC link or the IGBT Collector when the transistor is fully switched-on, from equation [3],

$$IGBT\text{ Collector Current, } I_C = \frac{3}{\Pi} \times \frac{V_{line[\max]}}{R}$$

Where, R is the total circuit resistance. For this calculation, it is required to consider the rotor internal resistance, resistance of the DC link commutating choke, resistance between collector and emitter terminals when transistor is fully switched-on, and the junction resistance of the diodes.

6.6 Transistor Chopper:

This is a First Quadrant Chopper and the load is the rotor winding of the WRIM. As the duty factor of the transistor increases average current flow through the chopper will increase and that cause to increase the rotor current of the motor. Meaning that as the rotor current increases the rotor speed will increase. Main component of the transistor chopper is the Insulated Gate Bipolar Transistor (IGBT). When selecting the transistor, it is required to consider the Collector Current (I_C) and the Maximum Collector to Emitter Voltage (V_{CE}). In here too, it is good practice to keep a safety factor to ensure a long reliable operation of the IGBT while minimizing the higher cooling requirements of the transistor. Figure 6.4 given below shows the equivalent circuit schematic and the actual figure of the IGBT Module selected.

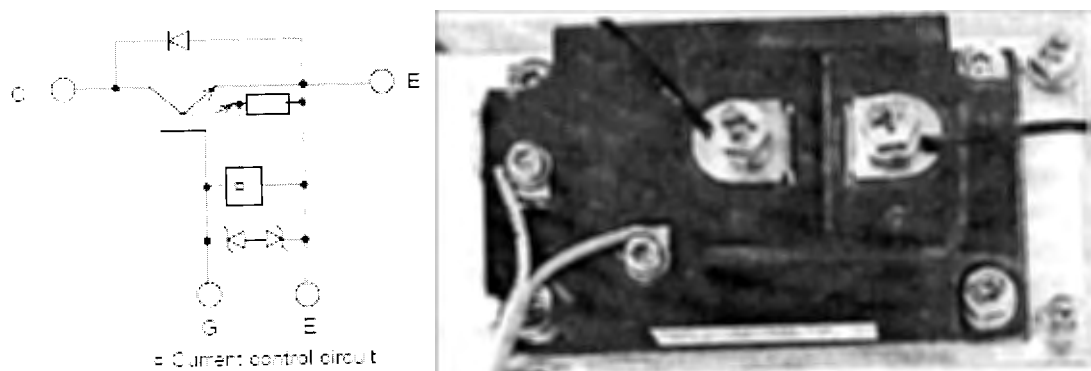


Fig-6.4: Equivalent Circuit Schematic and Actual Figure of the IGBT Module

6.7 Maximum Ratings and Characteristics of IGBT:

Table 6.2 shows below the maximum ratings and characteristics of the IGBT selected for the construction of the power electronics starter. [7]

Item	Symbol	Rating	Unit
Collector-Emitter voltage	V_{CES}	1200	V
Gate-Emitter voltage	V_{GES}	± 20	V
Collector current	Continuous	300	A
	1ms	I_C pulse	600 A
	Continuous	$-I_C$	300 A
	1ms	$-I_C$ pulse	600 A
Max. power dissipation	P_C	2100	W
Operating temperature	T_j	+150	$^{\circ}\text{C}$
Storage temperature	T_{stg}	-40 to +125	$^{\circ}\text{C}$
Isolation voltage	V_{is}	AC 2500 (1min.)	V
Screw Torque	Mounting	-	3.5 Nm
	Power Terminals	-	4.5 Nm
	Control Terminals	-	1.7 Nm

Table-6.2: Maximum Ratings and Characteristics of IGBT

6.8 Snubber Circuit:

Snubber circuits can reduce the electrical stresses of power semiconductors into safe levels. There are different type Snubber circuits and are of capacitors (C), resistors (R), inductors (L), and diodes (D). In this case, RCD Snubber [11] is in place across the power terminal of the IGBT. Snubber circuits are used to protect transistors by improving their switching trajectory, and they are turn-off Snubber, turn-on Snubber and over voltage Snubber. For the gate terminals of the transistor won't receive ideal square wave signal to turn-on and off. In real world applications we can see a reasonable rising and falling times at the gate terminals of the transistor. This rise and falling times are subjected to deviate and alter the current and voltage waveforms, which flow through the power terminals from the ideal as explained in the figure 6.5 below. [8]

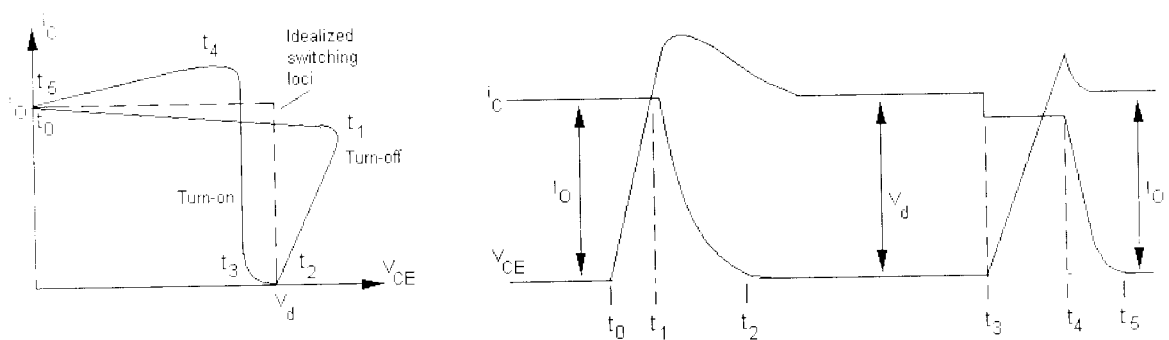


Fig-6.5: Switching Trajectory of the Gate Terminal and Current and Voltage Waveforms during Turn-On and Off

6.9 DC Link Commutating Choke:

The importance of having a DC link-commutating choke for the rotor circuit has been proved via simulations in the chapter 5 above. This could minimize the switching stresses on the rotor and stator current profiles. The feasible size of the inductor is 1-10mH ranges and for the final simulations 1mH has selected with higher switching frequency of the transistor, because the physical size of the inductor will increase as the inductance goes high. Figure 6.6 shows below a photograph of DC-link commutating choke.



University of Moratuwa, Sri Lanka.
Electronic Theses & Dissertations
www.lib.mrt.ac.lk

6.10 External Resistor:

As in the case above, the requirement of having external resistors and its function with the ohmic value are explained via simulations in the chapter 5 above. The used resistors are for practical implementation is high pulse ceramic resistors, which can allow flowing very high currents. Figure 6.7 is showing an actual photograph of high pulse ceramic resistors available in the power electronics starter of 11kW WRIM.



Fig-6.7: Start Connected External High Pulse Resistors

Chapter 7

IGBT Gate Driver and Control Unit

The IGBT Gate Driver unit sandwiches between the semiconductor based power block and the micro-controller based control unit. Hardware PWM signal generated by the micro-controller can't couple directly to the gate terminals of IGBT and it is needed to process electrically to suit for the transistor requirements. There are specifically designed semiconductor devices available for this and known as IGBT Gate Drivers. Figure 7.1 below shows an IGBT Gate Drive Optocoupler, and it is electrically isolated completely. Output of the driver is having a driving capacity up to 2.0A. Hewlett Packard manufactures this device and is HCNW3120. [9]

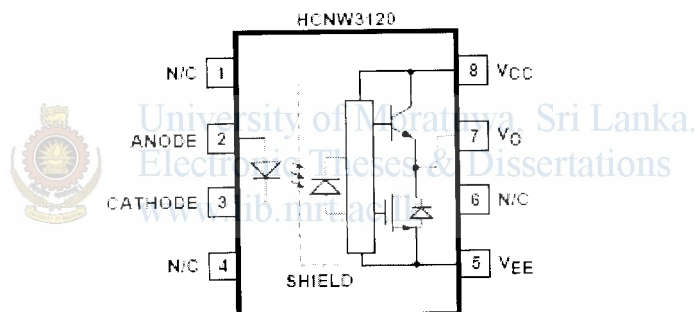


Fig-7.1: Schematic of the IGBT Gate Drive Opto-coupler

As the ratings of the IGBT increases the complexity of the gate driver circuit is also increases. The above HCNW3120 can be used up to 300A/ 1200V IGBTs, and when there is a higher version, it is recommended to use additional discrete stage at the output of the gate driver as shown in the figure 7.2 below.

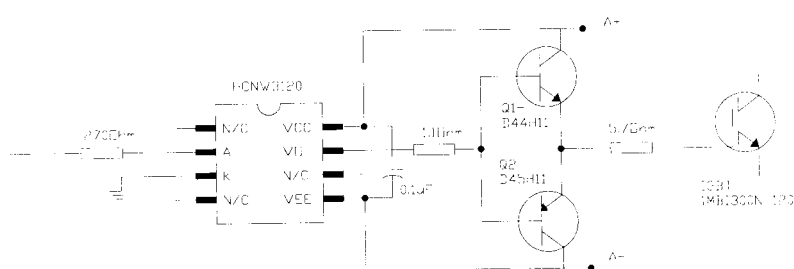


Fig-7.2: Schematic of an Optimized Gate Driver Circuit with Output Discrete Stage

Figure 7.3 shows below a gate driver with a discrete stage and it is for driving 800A/1600V IGBTs. It is used by very famous industrial VFDs by Siemens Germany. [10] But for our application, we do not require a very complex gate driver circuit, and an optimized gate driver circuit for the IGBT is given below in the figure 7.2 above.

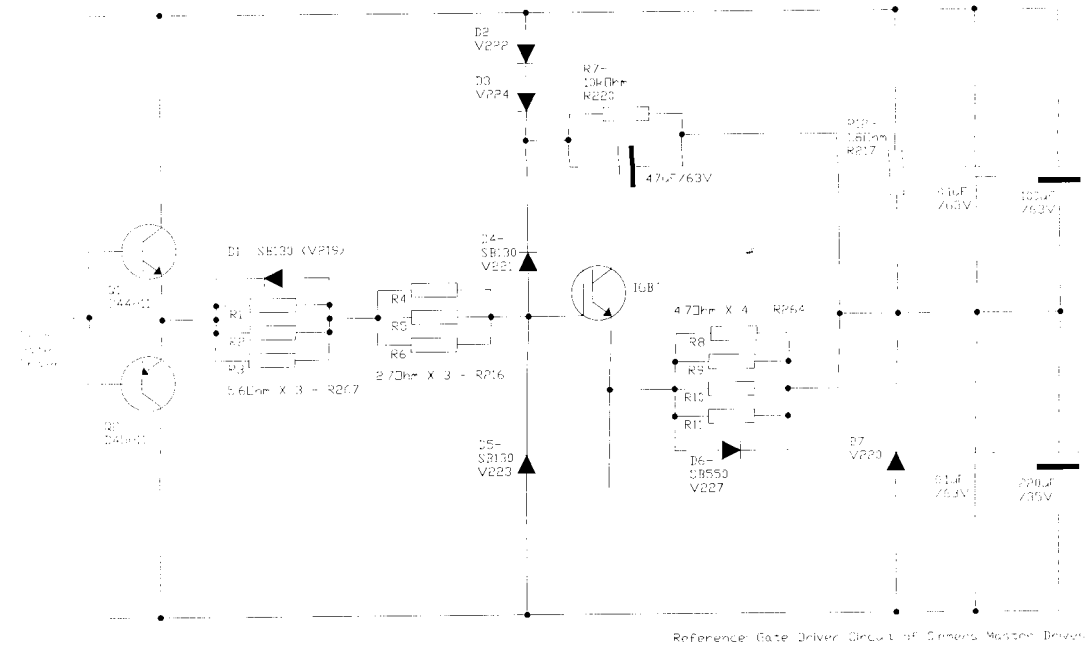


Fig-7.3: Schematic Diagram of an IGBT Gate Driver for Industrial VSD

7.1 Calculation of Gate Resistance:

Calculation of gate resistance is very important for the optimum operation of the IGBT and this will match the characteristics of the gate driver and the Gate terminal the IGBT. This can optimize the Rise-Time and Fall-Time of the gate driver signal, and consequently can minimize the power loss due to switching.

An example gate resistance calculation is given below in the figure 7.4. [9] According to the practical implementation, $V_{CC}=15V$ and $V_{EE}=0$.

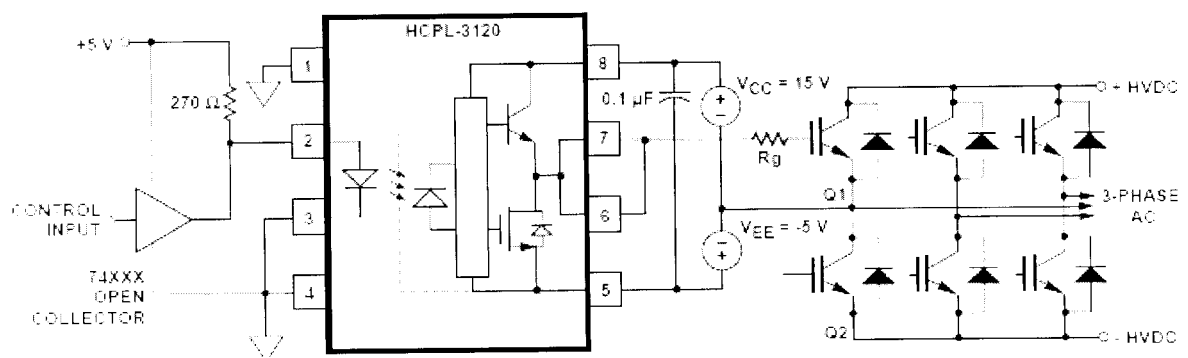


Fig-7.4: Gate Resistance Calculation of the IGBT

$$Rg \geq \frac{(V_{CC} - V_{EE} - V_{OL})}{I_{OLPEAK}}$$

$$Rg = \frac{(V_{CC} - V_{EE} - 2V)}{I_{OLPEAK}}$$

$$Rg = \frac{(15V - 0 - 2V)}{2.5A}$$

$$Rg = 5.2\Omega$$

According to the above calculation, the gate resistance for the driver is 5.2Ω .

7.2 Characteristics of the Gate Driver:

Figure 7.5 shows below the Gate driver signal, which is captured with an oscilloscope. Pulse frequency is 5kHz, peak-to-peak voltage of the signal is 14.4V and the mean voltage is 9.73V.

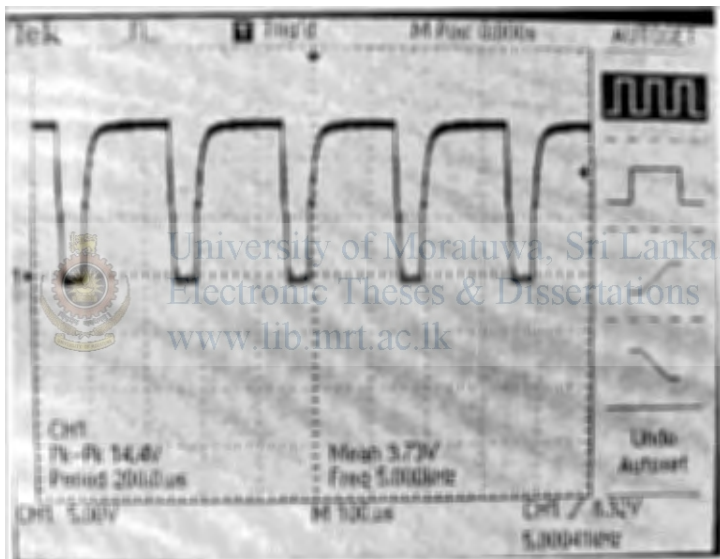


Fig-7.5: Waveform of V_{GE} - PWM Signal for IGBT

When it's come to the characteristics of the gate driver, Rise-Time and Fall-Time are very important. With the implemented circuit as in the figure 7.2 above, it is possible to achieve the rise time is 17.51us and the fall time is 8.967us at a pulse frequency of 5kHz.

Figure 7.6 and 7.7 below are showing the rise time and fall time waveforms captured by an oscilloscope. These characteristics are well suited for the IGBT and ensured a reliable and very effective gate driving by the design.

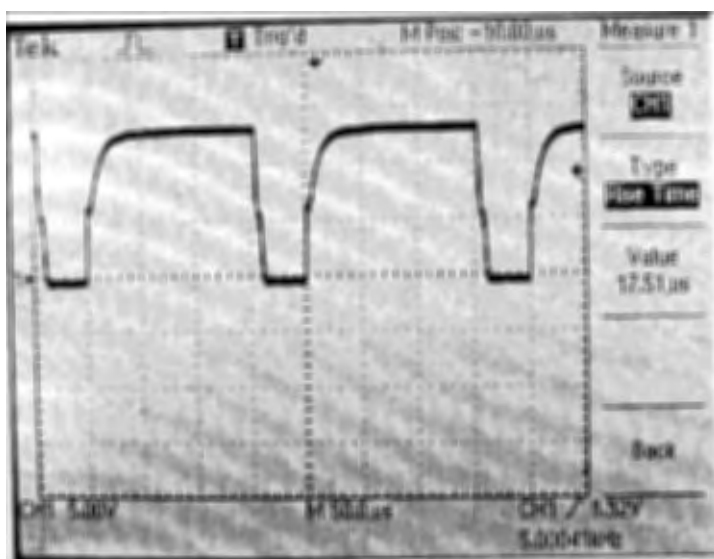


Fig-7.6: Rise Time Calculation of Gate Signal of IGBT with the Oscilloscope

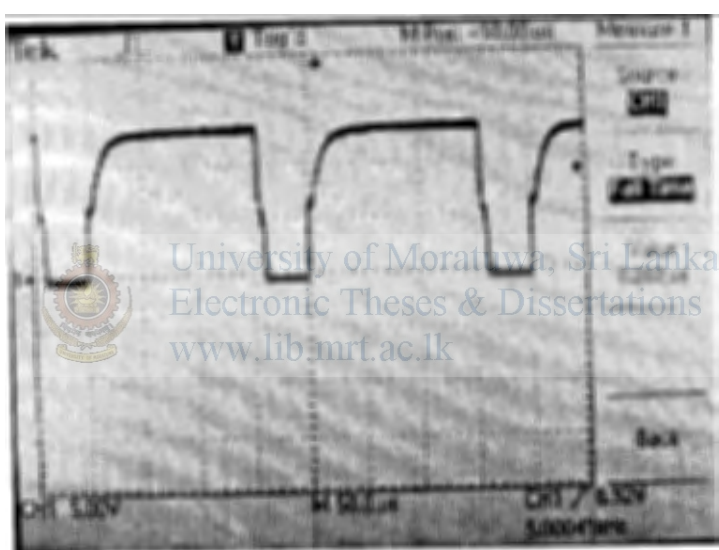


Fig-7.7: Fall Time Calculation of Gate Signal of IGBT with the Oscilloscope

7.3 Control Unit:

Central processor for the control unit is the PIC16F877A micro controller. It is having two Hardware Pulse Width Modulation (HPWM) outputs and one is used to drive the IGBT of the power electronics starter. This HPWM channel is having a facility to program the pulse frequency from 500Hz to 37kHz, but most preferred operating frequency is 10kHz and it has proven via simulations.

This includes an LCD to display the operating and programming data, and the controller parameterization can be done via a keypad. Further this is having a facility to program a Ramp-up time, which could be able to accelerate the rotor to the rated speed automatically within that given time. Reduction of the speed or the rotor to a minimum while stopping is also possible with this unit and it is called as the Ramp-down time.

Further, this control unit can be extended to control the speed of the rotor with a feedback loop, and the most concern disadvantage of the wound rotor motors with conventional starters can be fully omitted. Meaning that, this control unit can be extended to program the torque/ speed characteristics of the rotor or the load.

Figure 7.8 shows the schematic diagram of the control unit with the micro controller. And it is showing the electrical connection of the gate driver unit with the micro controller.

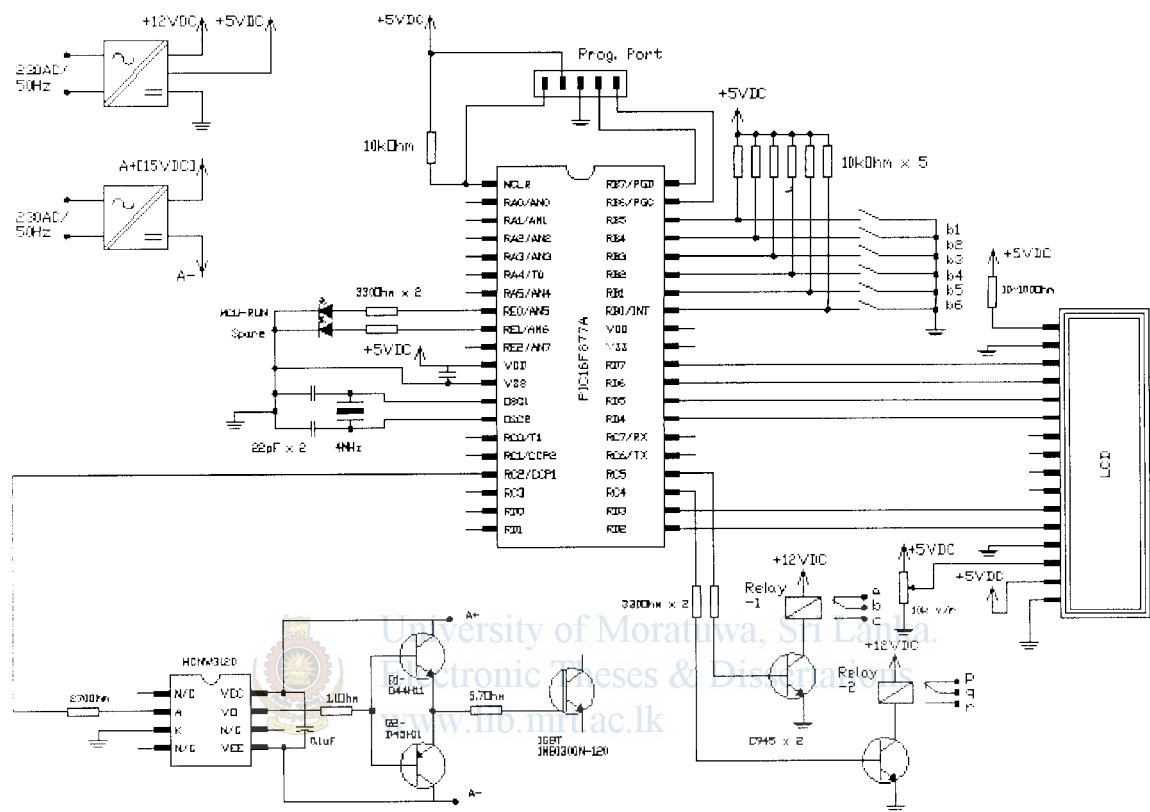


Fig-7.8: Schematic Diagram of the Control Unit for the Power Electronics Starter of WRJM

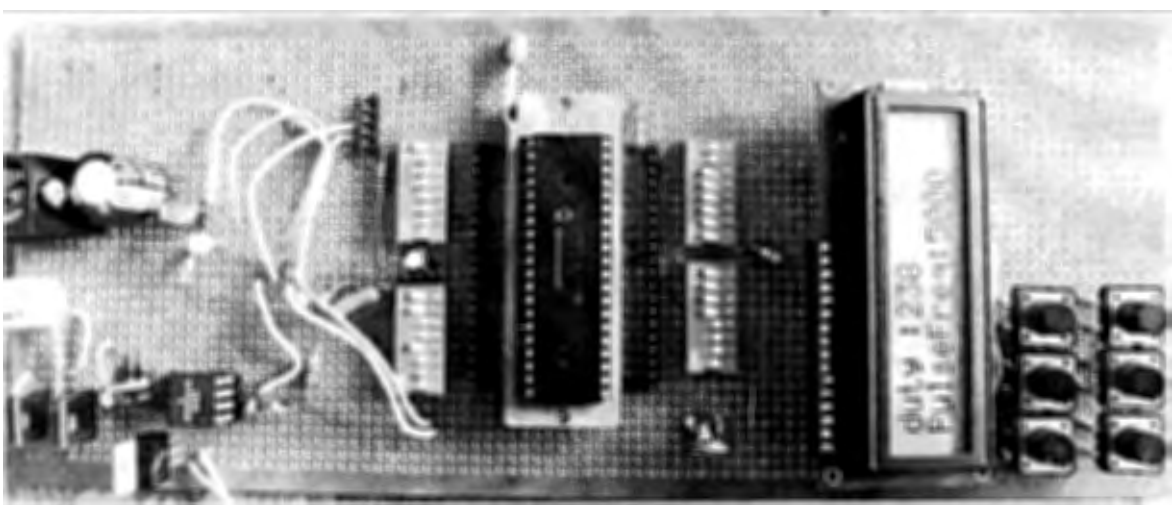


Fig-7.9: Actual Figure of the Control Unit for the Power Electronics Starter of WRIM

Additionally this unit is having two programmable relay outputs, which can extend to drive the stator power contactor and the bypass contactor for the rotor circuit as in the figure 3.1 above.

Actual photograph of the constructed control unit is shown in the figure 7.8 above. It is showing a duty of 238 out of 255 for the transistor gate drive at a pulse frequency of 5kHz.

7.4 Source Code for HPWM Waveform Generation:

Here the main Control unit is the PIC16F877A, a very famous micro-controller in the market. It is having 2 number of HPWM channels, and one channel is dedicated to drive the IGBT. Source code has developed to change the pulse frequency from 500Hz to 37kHz and the duty factor of the IGBT can control from 0 to 255, i.e. 8-bit resolution.

Liquid Crystal Display (LCD) unit is there for the display purposes, and a keypad is there to input parameters of the starter. Developed source code for the experiment is attached below, and is developed by using PICBASICPRO, which is readable very much.

```
ADCON1=%00001001
TrisE=0
TrisB=255
option_reg=0
on interrupt goto isr

intcon=%10011000

DEFINE LCD_DREG PORTD
DEFINE LCD_DBIT 4
DEFINE LCD_RSREG PORTD
DEFINE LCD_RSBIT 2
DEFINE LCD_EREG PORTD
DEFINE LCD_EBIT 3
DEFINE LCD_BITS 4
DEFINE LCD_LINES 2

pause 100
LCDOUT $FE,1,"Hello"
LCDOUT $FE,$C0,"World"

on_sw var bit
off_sw var bit
enter_sw var bit
on_sw=0
off_sw=0
enter_sw=0
duty var byte
duty=1
frequency var word
frequency=500

'enter var portB.0
function var portB.1
up var portB.2
down var portB.3
'on_sw var portB.4
'off_sw var portB.5
high portE.1

main:
if up=0 and duty<> 255 then
duty=duty+1
LCDOUT $FE,1,"duty :",dec duty
```

```

LCDOUT $FE,$C0,"PulseFreq:",dec frequency
gosub set_pwm
pause 200
endif

if down=0 and duty<> 0 then
duty=duty-1
LCDOUT $FE,1,"duty :",dec duty
LCDOUT $FE,$C0,"PulseFreq:",dec frequency
gosub set_pwm
pause 200
endif

if function=0 then
LCDOUT $FE,1,"function"
pause 200
endif

goto main

set_pwm:
HPWM 1,duty,frequency      ' Send a 50% duty cycle PWM signal at 1kHz
return

disable
isr:
if intcon.0=1 then      'Portb pin change interrupt
intcon.0=0

    if portb.4=0 then
        on_sw=1
        if frequency <> 25000 then
            frequency=frequency+50
            LCDOUT $FE,1,"pulsefreq:",dec frequency
            HPWM 1,duty,frequency
            pause 200
        endif
    endif

    if portb.5=0 then
        off_sw=1
        if frequency <>500 then
            frequency=frequency-50
            LCDOUT $FE,1,"pulsefreq:",dec frequency
            HPWM 1,duty,frequency
            pause 200
        endif
    endif

endif

if intcon.1=1 then      'RBO interrupt
intcon.1=0
enter_sw=1
LCDOUT $FE,1,"enter_sw"
pause 500
endif

resume
enable

end

```

Chapter 8

Results and Discussion

Main focus of this chapter is to produce results of power electronics starter with its successful run with WRIM. Power electronics starter has shown very successful results as a starter and can act as a variable speed drive for a limited speed range. When it's come to the variable speed operation, the proposed power electronics starter cannot vary the speed of the rotor as a VFD does, because by design we are feeding the rated voltage and frequency to the stator of the motor directly. But even though, this starter shows a very appreciable speed control for a certain region, and it is not the full range as from zero speed to rated speed. The initial speed of the rotor will determine by the external resistance connected to the rotor winding, and speed control from that initial speed to the rated speed can be achieved via the proposed power electronics starter very smoothly.

Figure 8.1 below shows an actual photograph of measuring of rotor speed with a digital tachometer during its practical test.

University of Moratuwa, Sri Lanka.



Electronic Theses & Dissertations

www.lib.mrt.ac.lk



Fig-8.1: Measuring Rotor Speed with a Digital Tachometer

The table 8.1 below shows the recorded data during the tests with power electronics starter. It shows very clearly, the proposed power electronics starter can vary the rotor speed with the duty factor of the transistor, and with the increase of duty factor, the current flow through the IGBT increases and current flow through the external resistor reduces. At the maximum speed of the rotor or the 100% duty factor of the transistor, the current flow through the external resistor is zero and it has fully bypassed by the IGBT.

IGBT Current (A)	Ext Resistor Current (A)	V _{CE} (V)	RPM	Duty Factor (D)
0	1.5	72	365	0
0.66	0.6	51.6	401	25
0.88	0.5	47.4	433	50
1.17	0.5	42	468	75
1.34	0.4	35.5	508	100
1.58	0.3	30.6	539	125
1.84	0.3	25.95	569	150
2.1	0.2	21.36	596	175
2.48	0.2	16.1	629	200
2.71	0.1	10.33	666	225
3.82	0	0.66	729	255

Table-8.1: Measuring of IGBT Collector Current, Current through External Resistor, V_{CE} and Rotor Speed vs. Duty Factor

University of Moratuwa, Sri Lanka.

Figure 8.2 shows below a graph of Rotor Speed and V_{CE} of IGBT vs. Duty factor of the IGBT. Initial speed with external 33Ohm star connected resistor bridge is about 365rpm. And the rest of the speed has controlled via the power electronics starter. It shows an almost linear speed increase with the duty factor and at a duty factor of 100%, it reaches to the rated speed.

Initially the IGBT is fully opened and the VCE shows the developed voltage at the DC link by the rotor winding with externally connected resistors, and at a duty factor of 100%, the VCE is 0.66V, meaning that the transistor is fully switched ON.

All the tests have been carried out with a no load 11kW WRIM. The same tests can be extended with a loaded motor in future. The main disadvantage of the conventional external resistance starter of the WRIM is resistance changes are done in step by step with pre defined values and hence the speed variation and current flow though the motor are not smooth. Therefore the rotor speed at a certain external rotor resistance is highly depending on the load torque. In simple terms as the load torque varies, the rotor speed can vary even with the same external resistance.

But with this power electronics starter, we can avoid that main disadvantage, as the speed controlling is possible with the duty factor of the IGBT. To achieve the speed regulation irrespective to the load torque, it is required to have a closed loop speed control operation with this power electronics starter. Further discussion on this subject will present in the chapter 9.

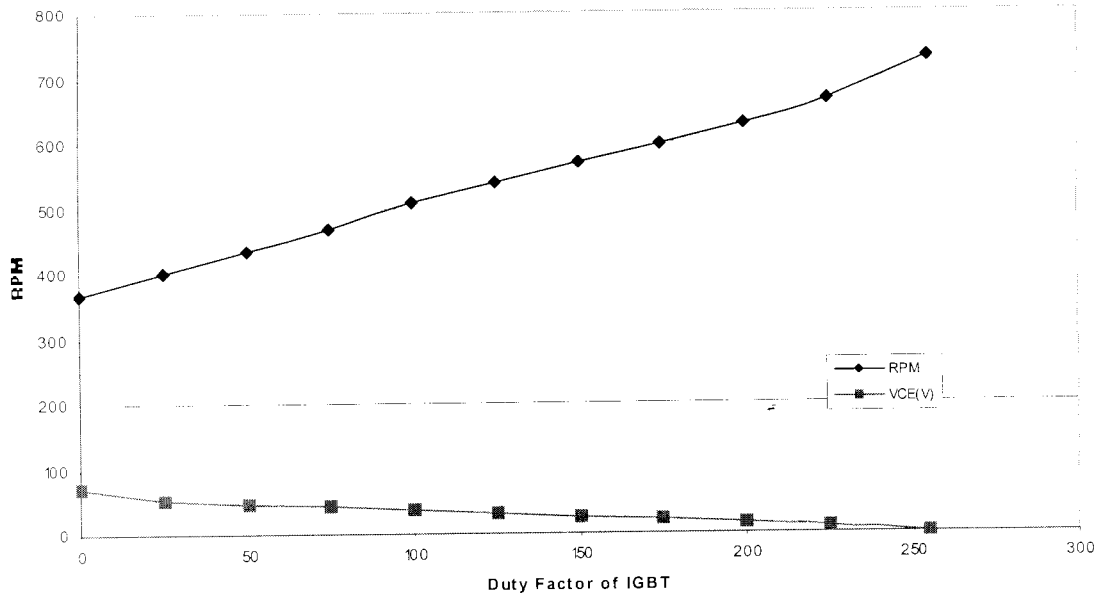


Fig-8.2: Rotor Speed and V_{CE} vs. Duty Factor of IGBT

Figure 8.3 below shows the behavior of current flows through the external resistor and the IGBT with the increased duty factor. Initial whole rotor current will flow through the external resistor as the IGBT is fully turned off. As the duty factor increases, current flow through the external resistor reduces and current flow through the IGBT increases. At a duty factor of 100% or as the IGBT is fully turned on, the whole current will pass through the collector of IGBT, and flow through the external resistor will be zero.

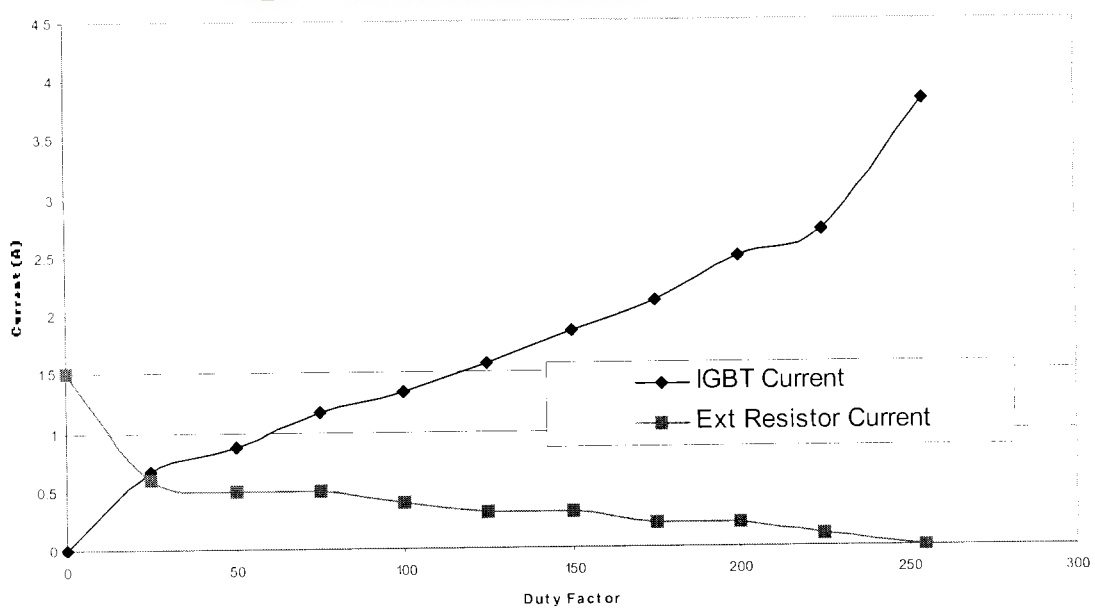


Fig-8.3: Current through IGBT and External Resistor vs. Duty Factor of IGBT

8.1 Analysis of Rotor Currents:

Figure 8.4 shows below the rotor current profile only with the external resistors, and the duty factor of the transistor is zero. Rotor current will follow a sinusoidal pattern as the figure shows. Small distortions are available for the waveform as the experiment carried out in a highly industrial environment.

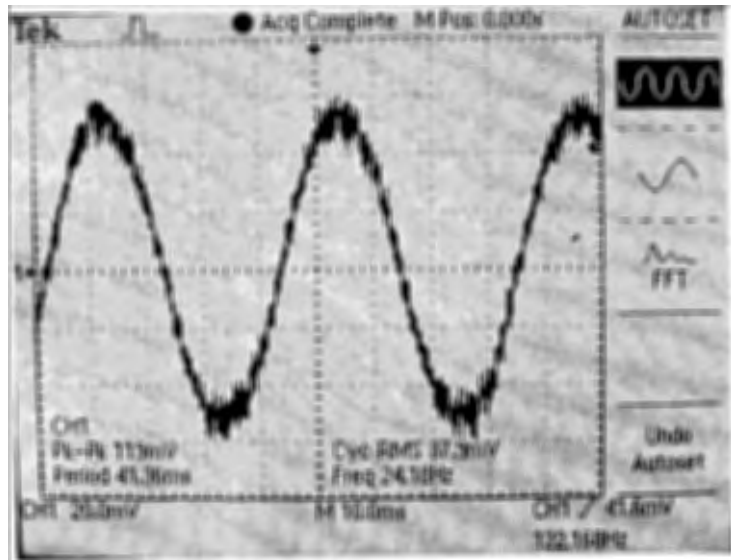


Fig-8.4: Rotor Current Profile with External Resistance

Figures below show the rotor current profiles at different duty factors and pulse frequencies. Figure 8.5 shows the rotor current profile at a duty factor of 20% and a pulse frequency of 5kHz. As the IGBT starts to switch, rotor current profile will deviate from the sharp sinusoidal pattern.

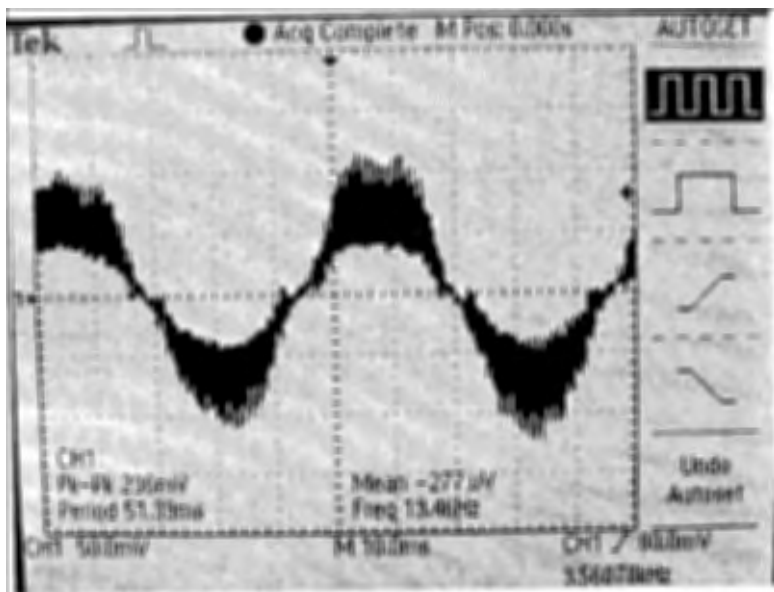


Fig-8.5: Rotor Current Profile at 20% of Duty Factor and Pulse Frequency of 5kHz

Figure 8.6 shows the rotor current profile at a duty factor of 40% and a pulse frequency of 5kHz.

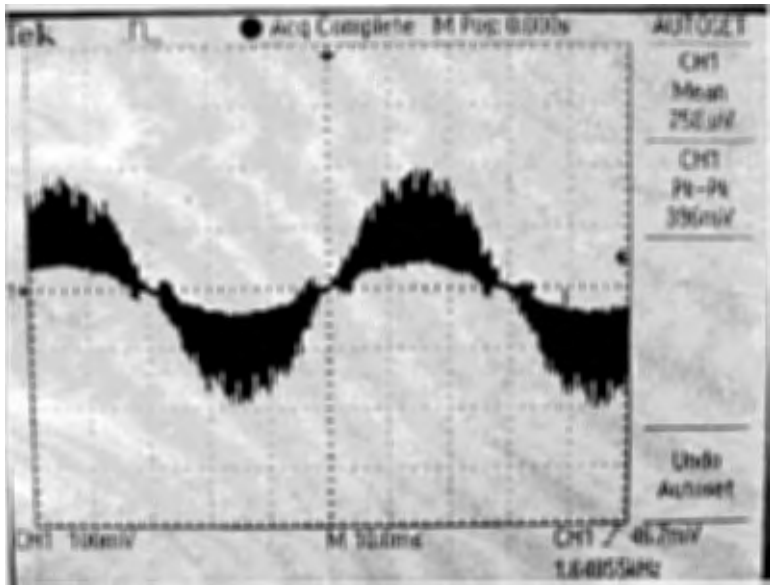


Fig-8.6: Rotor Current Profile at 40% of Duty Factor and Pulse Frequency of 5kHz

Figure 8.6 shows the rotor current profile at a duty factor of 80% and a pulse frequency of 5kHz. As the duty factor increases, the rotor current will approach to the original sine wave.

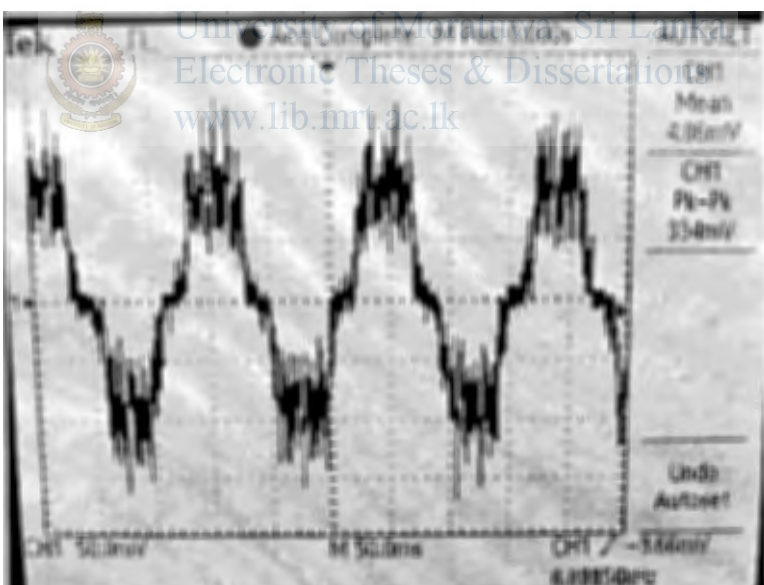
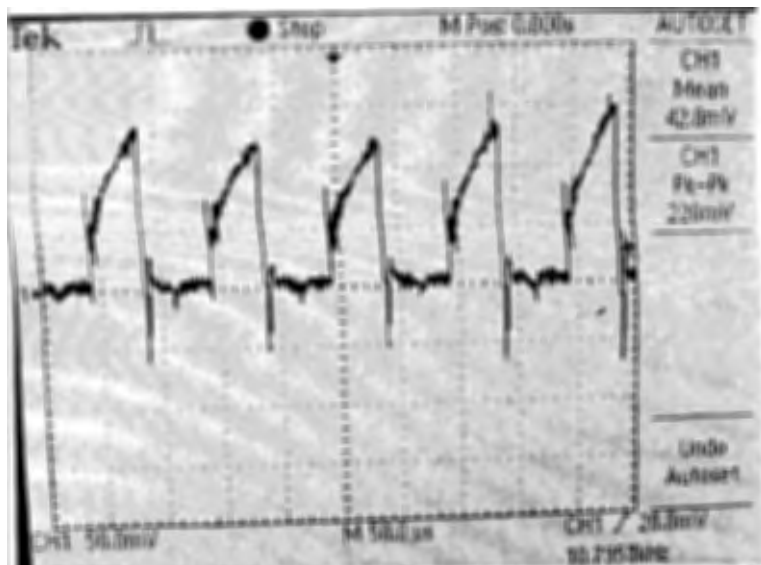


Fig-8.7: Rotor Current Profile at 80% of Duty Factor and Pulse Frequency of 5kHz

8.2 Analysis of Currents Waveform through the DC Link Commutation Choke:

DC Link commutation choke minimize the switching stresses on the rotor winding. Figure 8.8 shows below the current profile via the DC Link commutation choke at a duty factor of 40% and a pulse frequency of 10kHz. As the oscilloscope calculates, the mean voltage drop across the inductor for a no load motor is about 42.5mV, and this ensures a very small

power loss at the inductor. But as the motor load increases this will increase. For the current measurement, oscilloscope probe connected across a 0.05Ohm resistor, and hence we can calculate the average current flow through the inductor, and is 0.856A.



*Fig-8.8: Current Profile through the DC Link Commutation Choke
at 40% of Duty Factor and Pulse Frequency of 10kHz*

Maximum power loss across the inductor can analyze at a maximum duty factor of the transistor. Figure 8.9 shows below the current profile via the DC link commutation choke at a duty factor of 100% and at a pulse frequency of 10kHz. Here the mean voltage across the choke is 134mV across a 0.05Ohm resistor. Therefore we can calculate the average current flow through the inductor, and is 2.68A for a no load motor.

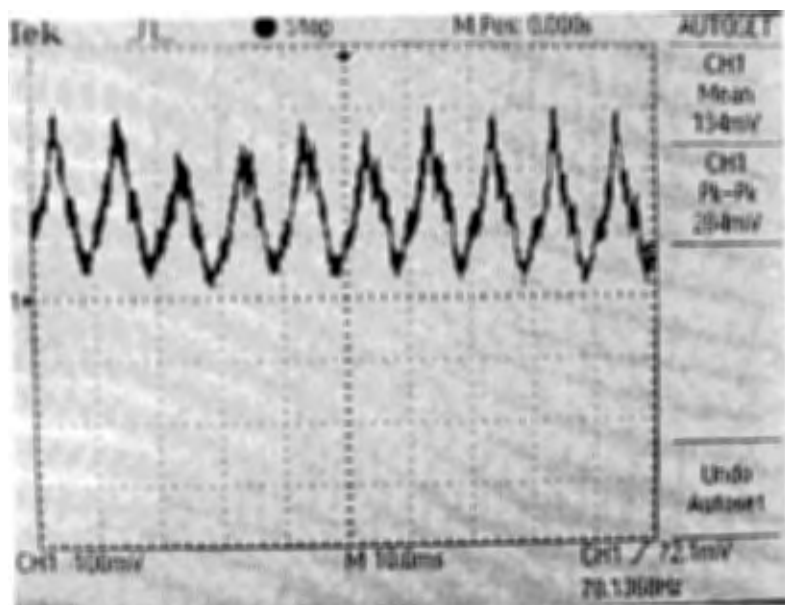


*Fig-8.9: Current Profile through the DC Link Commutation Choke
at 100% of Duty Factor and Pulse Frequency of 10kHz*

8.3 Harmonic Analysis:

A Fluke 43B Power Quality Analyzer (PQA) is used to analyze the harmonics generated due to power electronics starter. As the power electronics starter operates at a higher switching frequency, it is advisable to investigate the harmonic generation by that starter. Figure 8.10 shows the PQA in connection with the WRIM.



Fig-8.10: Electrical Connections of the Fluke Analyzer with WRIM

Table 8.2 shows the Total harmonic Distortion (THD) vs. the duty factor of the IGBT at a pulse frequency of 5kHz. THD increases as the duty factor increases, and recorded a maximum distortion at a 100% duty factor of the transistor.

Switching Frequency	Duty of IGBT	THD%	Current (A) rms
5kHz	0	0.4	7.06
5kHz	50	0.5	6.99
5kHz	100	0.6	7.06
5kHz	150	0.7	6.99
5kHz	200	0.9	7.02
5kHz	255	2.2	6.84

Table-8.2: Harmonic Analysis at Different Duty Factors and Pulse Frequency of 5kHz

Further, we have changed the base frequency or the pulse frequency from 0.5kHz to 10kHz and observe the THD value at the maximum duty factor. THD value is almost same and keeping constantly as the base frequency changes.

Switching Frequency	Duty of IGBT	THD%	Current (A) rms
0.5kHz	255	2.3	6.87
1kHz	255	2.4	6.9
2.5kHz	255	2.3	6.87
5kHz	255	2.2	6.84
7.5kHz	255	2.1	6.77
10kHz	255	2.3	6.84

Table-8.3: Harmonic Analysis at different Pulse Frequencies

When we having a closer look on the harmonics generated by the power electronics starter, the highest recorded THD value is 2.4%, and it is well within the acceptable range. But it is important to notify, the analysis has done for the no loaded motor, and future studies will complete the harmonic analysis with a loaded motor.

Figure 8.11 shows a recorded figure during the harmonic analysis with the PQA at a 100% duty of the IGBT and a pulse frequency of 5kHz. This shows 3rd and 5th harmonics are originated slightly, and not significantly.

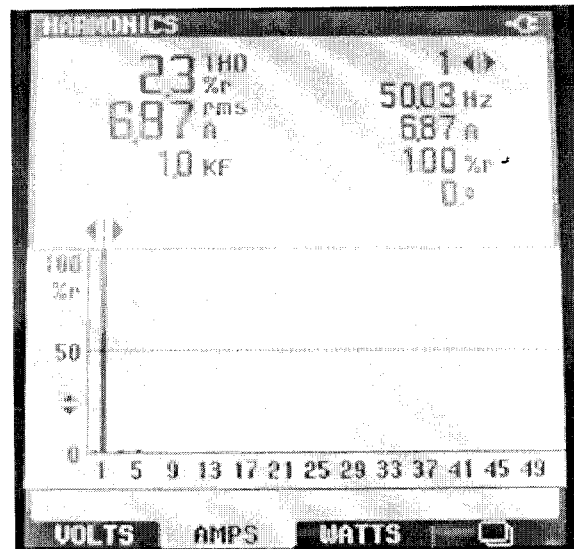


Fig-8.11: Harmonic Analysis of WRJM at 100% of Duty Factor and Pulse Frequency of 5kHz

The proposed power electronics starter is a rotor-based starter and switching stresses will minimize by the DC link commutation choke and by the internal rotor inductance. Transfer of switching stress to the stator is at a lower value and the harmonic generation with a delta connected stator winding is at a very low level as the results shows above.

This implies that, there is a very low chance to generate a higher THD value with a rotor based power electronics starter as in the proposal.

Above THD measurements have been done, once the rotor speed becomes stable at a relevant duty factor of the IGBT. Further more it is advisable to observe the THD levels during the acceleration of the rotor under a pre-set ramp.

8.4 Analysis of Rotor Current Profiles with the FLUKE PQA:

Analysis of the rotor current profiles has been done with the FLUKE PQA too and it confirms the results obtained with the oscilloscope.

Figure 8.12 shows below the rotor current profile at 50% of duty factor and pulse frequency of 10kHz.

Figure 8.13 shows below the rotor current profile at 100% of duty factor and pulse frequency of 10kHz.

Figure 8.14 shows below the rotor current profile at 0% of duty factor and pulse frequency of 10kHz. Further more, this shows the initial current profile through the rotor only with the external resistors.

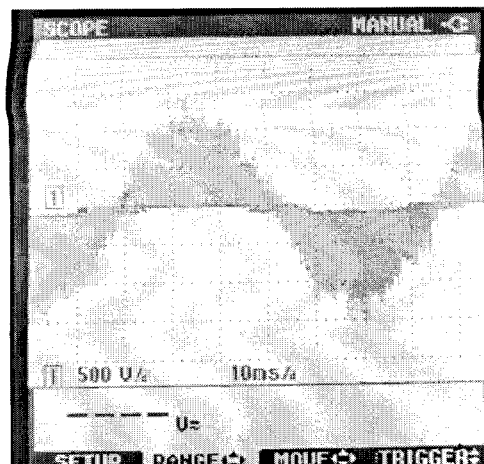


Fig-8.12: Rotor Current Profile at 50% of Duty Factor and Pulse Frequency of 10kHz

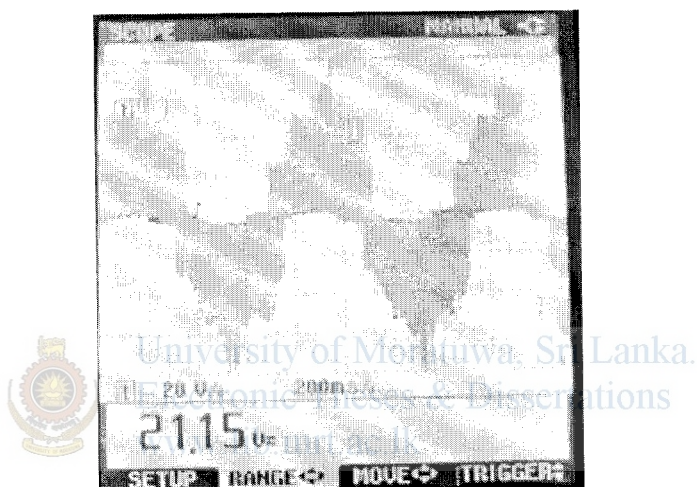


Fig-8.13: Rotor Current Profile at 100% of Duty Factor and Pulse Frequency of 10kHz

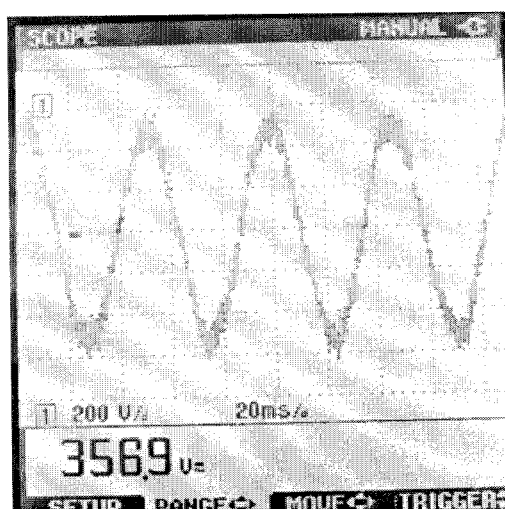


Fig-8.14: Rotor Profile at 0% of Duty Factor and Pulse Frequency of 10kHz

Chapter 9

Comparison, Reliability of the System and Further Improvements

This chapter focuses on the comparison of the performance of the power electronics starter vs. conventional rotor resistance starter, reliability of the power electronics starter and further developments possible.

9.1 Power Electronics Starter vs. Conventional Starter:

Figure 9.1 below shows a starting stator current profile of an 11kW WRIM with the proposed power electronics starter and the conventional rotor resistance based starter with the development of rotor speed. As the conventional starter changes rotor resistance by steps, stator current fluctuations are high, and the rotor acceleration is not constant over the time. But with the proposed power electronics starter, we can control the duty factor of the IGBT as per the requirement, and can achieve a smooth speed increase and thereby can achieve no current peaks and fluctuations at the stator. Figure 9.1 shows the captured stator current profiles of a no load motor.

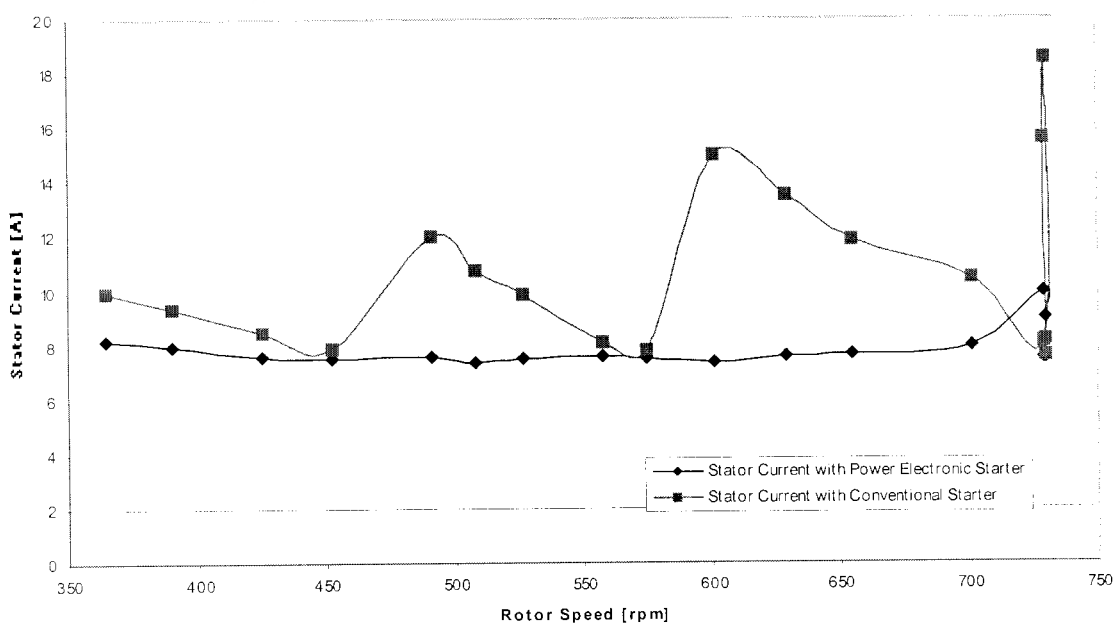


Fig-9.1: Stator Current Profiles vs. Rotor Speed of an 11kW no load WRIM

9.2 Reliability of the System:

Power electronics starter is having two basic units; they are a power block with power semiconductors, resistors and an inductor, and a control unit with a micro controller and other electronics. Entire design of the power electronics starter is based on the nameplate data of the WRIM and the application based information. Since this starter doesn't have rotating parts and electrical contacts as in the conventional starter, the reliability of the proposed starter is very high.

No need to maintain a bulky resistor based oil or air cooled starter, and minimize the maintenance. Practice in the industry to run a WRIM is to have two separate motor control circuits for the stator and the rotor starter separately, and with a suitable interlocking in between. This causes lot of troubles during the starting of the motor and if any control fails the damage would be severe and the time taken to diagnose and rectify is very high. But with this power electronics starter, we can handover the entire control of the WRIM to a single micro controller, and this could cover the control of both stator and rotor. This minimizes the field level hardwiring too.

In a conventional method all the protections are ensured for the WRIM via its stator circuit, but with this power electronics starter, we can introduce a secondary protection scheme to the rotor circuit also. This is nothing but an over-current protection and it could detect loose connections at the slip rings and locked rotor situations very fast and further provide a safe operation for power semiconductors in the power block.

9.3 Programmable Torque-Speed Characteristics:

The proposed power electronics starter can avoid the main disadvantage of the rotor resistance starter, which is the rotor speed dependability over the load torque. The design of the proposed power electronics starter can be extended to a closed loop speed control and hence can achieve the programmable torque speed characteristics. Figure 9.2 below shows the extension of the proposed power electronics starter to have a closed loop speed control.

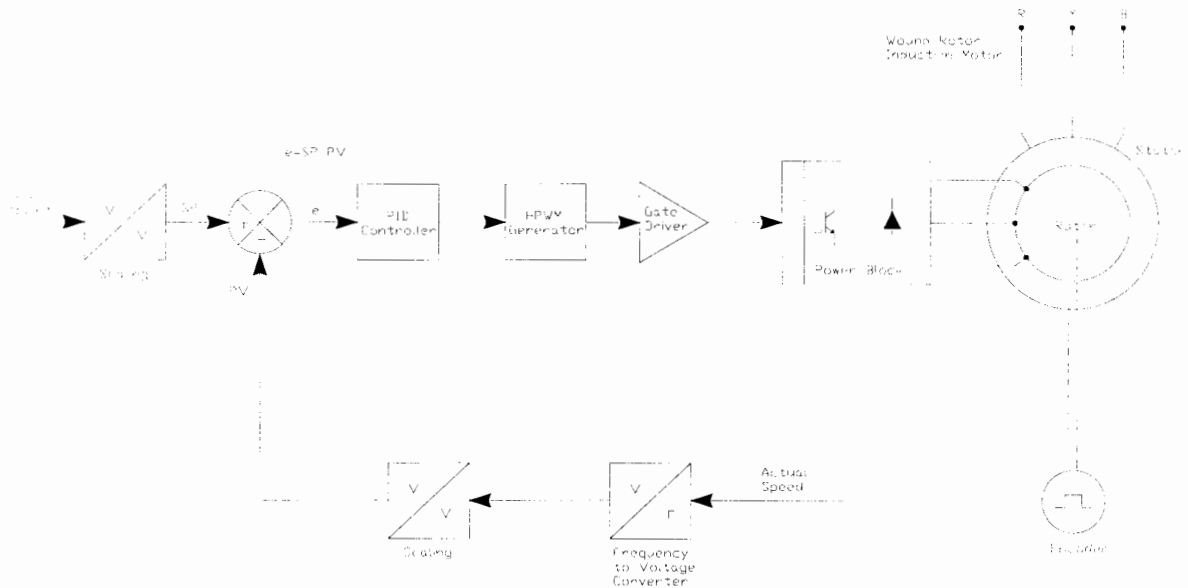


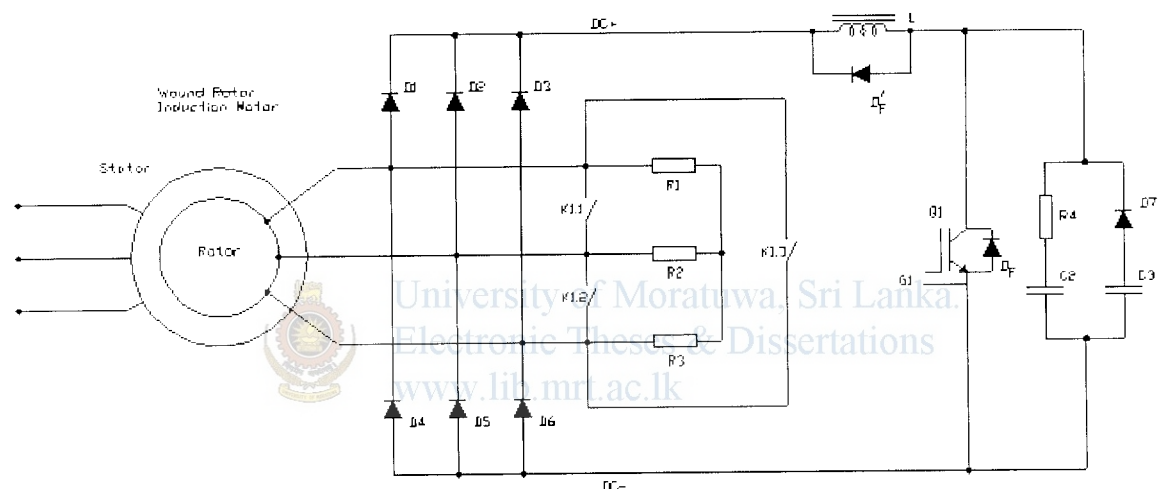
Fig-9.2: Closed Loop Speed Control of a WRIM with Power Electronics Starter

For the speed control of a WRIM, it is required sense the actual rotor speed (PV) via an encoder, and the speed error can be detect with respect to the set speed or the reference set point (SP). This error can compensate via a PID controller, which can derive the magnitude of the duty factor for the transistor.

This closed loop speed control ensures the accuracy in the rotor speed irrespective to the load torque. With the conventional methods, it is impossible to have a closed loop speed control and thereby it is unable to have a programmable torque speed characteristics.

9.4 Integration of Freewheeling Diode across the DC Commutation Choke:

The original proposal doesn't contain a freewheeling diode across the DC commutation choke. Since it is performing as an inductor, the stored energy of the inductor should be dissipated during the off state of the IGBT. When the freewheeling diode of the inductor (D'_F) was not in place, R4 and C2 compound of the snubber circuit will circulate the reverse energy of the inductor when the IGBT switches off. Anyhow this freewheeling diode should be a fast recovery diode with a higher current handling capacity.



Ratings of the fast recovery diode can be calculated as follows.

$$V_L = L \frac{di}{dt}$$

Let the current through the freewheeling diode (D'_F) is i_F , that can be limited by the summation of the internal resistance of the diode and the inductor, (R'_F).

$$i_F = L \frac{V_L}{R'_F}$$

i_F would be the forward current handling capacity of the diode and the PIV of the diode should be greater than the V_{DC} . i_F can be limited to a safe value by introducing a suitable resistance in series with the diode.

9.5 Advantages and Disadvantages of Power Electronics Starter over Conventional Starter:

Power electronics starter is very simple by construction and can be extended to its function as a speed controller in addition to a starter. Programmable speed increase and decrease are possible within a pre-set time period. Entire control of a WRIM can be incorporated to a single micro controller and secondary level rotor circuit protection can be achieved by sensing rotor currents.

The proposed starter is required very few power electronics semiconductors and the cost for the development will be the same as the conventional rotor resistance starter.

Minimizing the electromechanical connections and the rotating parts by the new design can improve the reliability and the availability of the WRIM, and requires a very low maintenance effort.

9.6 Advantages and Disadvantages of Power Electronics Starter over Variable Frequency Drive:

Investment is low for a power electronics starter as it compares with a variable speed drive. But speed control is more precise from zero speed to the rated or above. With the proposed power electronics starter, the speed control range is limited by the external resistors connected to the rotor circuit, and cannot go beyond the rated speed. Reversing of the rotor turning direction and electronics braking are not possible with the power electronics starter. Harmonic generation is very as it compares with a VFD and expertise knowledge is not required for commissioning the power electronics starter to a WRIM.

9.7 Conclusion:

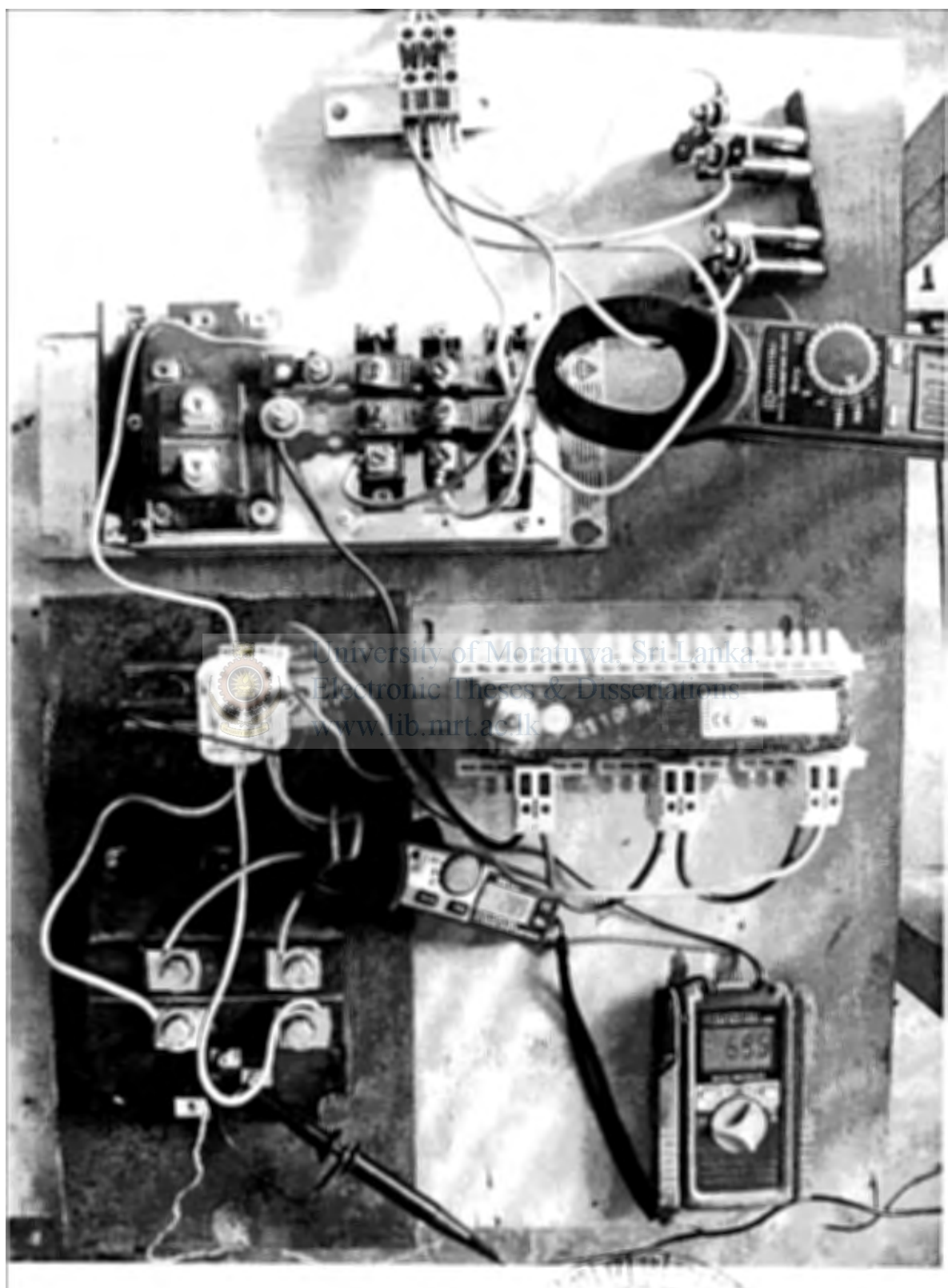
The proposed power electronics starter is a very successful replacement to a conventional rotor resistance starter. It could save the space requirement and can minimize the cooling requirement of the resistive starter. Conventional starter limits the number of consecutive start-ups, but the proposed power electronics starter is having a continuous duty, and can achieve a very smooth speed control of the rotor from the initial speed (speed due to external resistors) to the rated speed. Further this could replace the bulky resistor banks and other electromechanical parts. Minimizing the rotational parts will extend the reliability and requires a very low maintenance.

Further more, the proposed starter can avoid the rotor speed dependability over the load torque, and can extend the design easily to have programmable torque-speed characteristics.

References:

- [1] Wound RotorTM Motor Technology, TECO Westinghouse Motor Company
- [2] Induction Motor Parameters Extraction by Sinisa Jurkovic
- [3] Siemens MICROMASTER 440 - 0.12 kW - 250 kW, Operating Instructions, 6SE6400-5AW00-0BP0, Issue 07/05
- [4] Help, SimPowerSystems, Asynchronous Machine, Matlab-Simulink, Version-7.5.0.342 (R2007b), August 15, 2007
- [5] MDD 95-16N1 B, IXYS Diode Modules, 2000
- [6] Cyril W Lander, Third edition-1993, Power Electronics
- [7] Data Sheet for IGBT Module, 1MBI300N-120 by FUJI Electric
- [8] Power Electronics, Chapter 27, Snubber Circuits, pp.669, 681.
- [9] HCNW3120, 2.0 Amp Output Current IGBT Gate Drive Optocoupler by Hewlett Packard, Obsoletes 5965-4779E, 5965-7875E (7/97)
- [10] Siemens, MASTERDRIVESVC – IGD (Inverter Gate Drive) Card, Part No. 6SE7035-7GK84-1JC0
- [11] Siemens MASTERDRIVESVC – Snubber Circuit, Part No. 6SE7038-6GK84-1GF0
- [12] Dr. P.S. Bimbhra, Fourth edition-2006, (page number – 639 – 644)

Annex: Actual Figure of Implemented Power Electronics Starter



University of Moratuwa, Sri-Lanka
Electronic Theses & Dissertations
www.lib.mrt.ac.lk

2010
55